Determining the Damage State of the Electrical Distribution System Following an Earthquake

Rebecca Nicole Breiding

A thesis

Submitted in partial fulfillment of the

Requirements for the degree of

Master of Science in Electrical Engineering

University of Washington

2015

Committee:

Daniel Kirschen

Miguel Ortega-Vazquez

Program Authorized to Offer Degree:

Electrical Engineering Department

University of Washington

ABSTRACT

Determining the Damage State of the Electrical Distribution System Following an Earthquake

Rebecca Nicole Breiding

Chair of the Supervisory Committee:

Close Professor Daniel Kirschen

Electrical Engineering Department

Natural disasters are unpredictable in when and how strong they will be when they occur. This unpredictability makes determining how a system will react to the undesired input difficult. In addition, when a natural disaster strikes a populated area, the lifelines which support the area, water, electricity, etc., are all affected. These effects intertwine and affect the local populace, causing hardship and harm. The goal of this research was to attempt to reduce the harm done to the affected populace in the wake of a natural disaster. This research specifically looked at the natural disaster of earthquakes and how earthquakes can affect the electrical power distribution system. An algorithm was made, which creates an abstract graph of the electrical distribution system, relating the various components of the distribution system with the probability of damage state the component is in.

Table of Contents

Table of Figures

List of Tables

1. Introduction

Every day brings with it changes, both desired and undesired. Some changes are created by man, such as the erection of new buildings and roads. Other changes are introduced by nature, through natural disasters, such as hurricanes, and tornadoes. Both of these types of changes need to be planned and prepared for. Manmade changes are planned for throughout the project. For natural disasters, however, lifeline planners need to consider two courses of action. The first is how to make the system as robust and resilient as possible within economic and time constraints. The second is to determine how to recover the system as quickly as possible in order to reduce the harm done to affected population and to restore normalcy as quickly as possible. This project addresses the second course of action, how to reduce the harm to the affected population with regards to the electrical power system. It begins to address the question: how can we turn the lights back on faster after a natural disaster? This research specifically looked at the effects of an earthquake on the electrical power system, however, other natural disasters and their effects on the power system were researched as well.

In order to study how to efficiently repair and restore the electrical power system after a natural disaster, several ideas and concepts need to be explored first. The first is the idea of resiliency in general, the various definitions and views of the word, and which definition this research applied to the word resiliency. The second is if it is possible to prevent the power system from being affected by a natural disaster. If damage is unavoidable, then knowing how different natural disasters affect the various power grid components is essential. If some components are more susceptible to certain natural disasters than others, and a given area is also more susceptible to the same natural disaster, then in order to improve the resiliency of the electrical grid, those components should be the focus of improvement efforts. Understanding how the electrical grid status after a natural disaster affects a community must also be explored.

Knowing how a community relies on the various lifelines, such as communication systems, transportation systems, and electric power systems, and how these systems interact is critical to understanding which loads have priority repair status. A thorough assessment both the critical infrastructure and the socio-economic impacts is immensely complicated.

1.1. Resiliency: Definitions

Resiliency has many different meanings and definitions depending upon the application of the word. Resiliency can be defined as the size of the shock required to perturb a system from the normal operating state and speed at which the system recovers from the shock (Maliszewski & Perrings, 2012). Mili defines resiliency as how a system can "gracefully degrade its function by altering its structure in an agile way when subjected to a set of perturbations and how quickly the system will recover once the perturbations have ceased." (Mili, 2011). The National Infrastructure Advisory Council looks at resiliency from an infrastructure stability perspective, and defines resiliency as "the ability to reduce the magnitude and/or duration of disruptive events." (Berkeley & Wallace, 2010). The American Center for National Policy defines resiliency as "the ability to prepare and plan for, absorb, recover from or more successfully adapt to actual or potential adverse events." (Flynn & Burke, 2012). Ecologists define resilience as "a measure of the persistence of systems and of their abilities to absorb change and disturbance and still maintain the same relationships between state variables." (Ouyang, et al., 2012). The Department of Homeland Security, looking at the various terrorist threats to the United States, conceptualizes resiliency as "the capacity of an asset, system or network to maintain its function during or to recover from a terrorist attack or other incident." (Ouyang, et al., 2012) One of the bodies devoted to studying the effects of earthquakes on all infrastructure, the Multidisciplinary Center for Earthquake Engineering Research (MCEER), defines resilience as "the ability of the system to reduce the chances of shock, to absorb a shock if it occurs and to recover quickly after

a shock and re-establish normal performance." (Ouyang, et al., 2012) There are numerous other definitions and interpretations of the term resiliency depending upon the perspective of the field and person applying the word. For this project, resiliency is defined as "the joint ability of infrastructure systems to resist (prevent and withstand) any possible hazards, absorb the initial damage, and recover to normal operation" (Ouyang, et al., 2012), and the infrastructure system under scrutiny is the electrical power system.

1.2. Critical Infrastructure Systems

The continuity of the electrical power system is critical to many of the fundamental government, local, and public missions (Berkeley & Wallace, 2010). This system is defined as one of America's critical infrastructure systems. Each country has a different list of which infrastructure systems can be defined as critical, but in general, the following systems are listed: telecommunications, electrical power, natural gas and oil, banking and finance, transportation, water supply systems, government services, and emergency services. All of these systems are needed to achieve society's goals, and they are all interdependent. For example, when the power system experiences an outage, traffic lights and water supply pumping stations do not operate, and businesses and banks close. As another example of critical infrastructure interdependence, when communications systems are disrupted, this affects the control and situation awareness of the water and electrical services, causing failures due to lack of observability (Ouyang, 2014). There are many other interdependencies not listed here. The criticality of these systems is underlined by the needs of a nation. Those systems which a country labels as critical help attain a country's fundamental missions which typically include economic stability and growth, national security, public safety, and citizens' quality of life (Berkeley & Wallace, 2010). In order for community planners to determine what repairs to begin with in the event of a natural

disaster, they must first understand how natural disasters affect the lifeline, or critical infrastructure, systems.

1.3. Natural Disasters: Types and Effects

Without knowledge of how a system is affected by an undesired input, community planners have no way of making the system less affected and more resilient to the input. Table 1 lists natural disasters and their adverse effects to the electrical power system.

Table 1: Natural Disaster Effects on the Electrical Power System

Natural Disaster	Effect
Ice Storms	Downed transmission lines due to ice loading and/or strong winds[1] Damaged distribution poles due to ice loading and/or strong winds[1]
Hurricanes	Downed transmission lines due to airborne debris and/or strong winds[2] Damaged distribution poles due to airborne debris and/or strong winds[2]
Floods	Damaged substations, transformers, and/or underground distribution lines due to water seepage[3,4]
Tornados	Downed transmission lines due to ice loading and/or strong winds[1] Damaged distribution poles due to ice loading and/or strong winds[1]
Earthquakes	Damaged transformers due to inadequate anchorage during shaking[5] Damaged underground lines due to ground liquefaction[6] Damaged aboveground lines due to poles shaking in opposite directions[7] Damaged aboveground lines due high weight loading of distribution poles[8]

1. (Wong & Miller, 2010)
2. (Ouyang & Duenas-Osorio, 2014)
3. (Abi-Samra & Henry, 2011)
4. (Anon., 2013)
5. (Ersoy, et al., 2008)
6. (Eidinger & Tang, 2012)
7. (Kempner, 2007)
8. (Rudnick, et al., 2011)

As can be seen from the table entries, some natural disasters, such as tornadoes, are much more likely to affect the transmission system, which is not the focus of this research, as opposed to the distribution system. Transmission structures are spread out between cities, moving the power generated from a generation station to the demand site. A distribution system receives the energy delivered by the transmission system and delivers it to the various load sites. Distribution

systems are more densely constructed than transmission systems and carry a lower voltage rating. These two systems are affected by different natural disasters due to the locations where the natural disaster is most likely to occur. However, the results to the structures are the same, either a transmission tower or a distribution pole, damage is incurred which causes a loss of power to a populace.

As seen in Table 1, different natural disasters affect different components of the electrical power system. When a natural disaster strikes a community, both government and lifeline leaders must be ready to enact their contingency plans immediately. This allows leaders to reduce the amount of economic and civil losses incurred when the power system is down. In the United States, the adjusted annual losses due to weather related outages are estimated to have cost the United States economy an adjusted annual average of $18 billion to $33 billion between 2003 and 2012. This costs include lost output and wages, spoiled inventory, delayed production, and inconvenience and damage to the electric grid (Anon., 2013). Earthquakes, while fortunately less frequent than severe storms, are less predictable, and cannot be anticipated and prepared for in the same way. While emergency restorations to the electrical power grid have been accomplished quickly, taking one day after the 1994 Northridge earthquake and three days after the 1995 Kobe earthquake, total repair time and costs are high. The estimated direct costs for the Northridge earthquake were approximately $500 million and $4 billion for the Kobe earthquake. Neither one of these earthquakes are at the strength of the anticipated "big one" for the West Coast of the United States (Shinozuka, et al., 1999), the Kobe earthquake was registered as a Richter magnitude 7.2 earthquake (Anon., n.d.), while the Northridge earthquake was recorded as a 6.7 Richter magnitude earthquake (Lowry, 2014). It is anticipated a Richter

magnitude 9.0 earthquake could strike the West Coast of the United States along the Juan de Fuca fault which runs from northern California to southern Canada (Berman, 2014).

1.4. Community Planning

Communities prepare for natural disasters in multiple ways, depending upon the anticipated threats. To prepare for earthquakes, utility and transmission companies install components specifically designed for seismic activities (Kempner, 2013) (Heimgartner, 2014). For hurricanes and tornadoes, natural disasters which include high winds, poles and other structures are upgraded utilizing stronger materials, or cables are placed underground where affordable and practical (Anon., 2013). In addition, utilities can redesign wires which detach easier, reducing repair time for damaged lines, or by installing stronger, tree-branch resistant aerial cables. For those communities in flood plains or affected by storm surges, installing more waterproof barricades and flood pumps around equipment is vital to protect underground distribution circuitry as well as both above and below ground substations. All natural disasters could benefit from smart switches which can detect changes on the line and reduce the number of customers affected by an outage (ConEdison, 2013).

Apart from looking at how to make the parts themselves either less susceptible to the natural disaster, or more easily repairable after the natural disaster, several communities are looking at the power grid in an entirely different light, by breaking it apart into smaller pieces. Microgrids are an old concept being made new again, as the electric grid was originally designed as a set of microgrids. Over the years, to take advantage of economies of scale, each of these microgrids was combined, allowing the power companies to operate more efficiently, charge cheaper rates to their customers, and be able to withstand greater perturbations without substantial effects (Schneider, 2014). In an effort to make their communities more resilient to natural disasters, politicians and community planners are considering implementing a microgrid

system, either to immediately switch on and provide energy in an island state after the natural disaster has occurred until the big power grid can be restored or as a steady state solution for day-to-day operation. These microgrids being implemented post natural disaster would be formed from renewable power sources, such as solar arrays, being connected together, and providing power to the loads closest to them. Theoretically, if enough power was produced, a microgrid could power the entire area serviced by a substation. New Jersey is researching combined heat and power plants, which use fuel located on site. The heat created is captured and used to heat water or buildings, creating self-sufficiency and reducing failures due to the big power system (Lamonica, 2012).

The primary consideration of municipalities and utilities after a natural disaster is to restore the affected area to the pre-natural disaster state is the minimal amount of time. Sometimes, the pre-natural disaster state is unobtainable, and a new steady state is obtained. This research focuses on attaining the pre-natural disaster state in a minimal amount of time by determining the probable damage state various components the electrical distribution system are in post natural disaster based on soil conditions and the strength of the earthquake.

2. Problem Description

As stated earlier, this research focused on how to determine the probable damage state the distribution system is in following an earthquake in order to repair it more efficiently. The researchers wish to apply scientific rigor to the process which already occurs at a utility company when a natural disaster occurs. Out of this research, a more time efficient and cost effective repair process should be attained. Currently, after a natural disaster, crews concentrate on repairing the main feeder, or backbone, first. Then, the crews begin to work on the three phase taps and the loads associated with them, and finally working on the single phase taps. If the crew knows there is a priority load, such as a hospital or customer on life watch assistance on a particular feeder, the crew can use their professional judgment and prioritize repairs accordingly (Bustos, 2014). Each utility should have a contingency plan prepared to implement in the event of a natural disaster. Spare parts should be stocked in various locations around the utility's jurisdiction in order to allow crews access post natural disaster when the transportation infrastructure may also be damaged and travel restricted (Bustos, 2014) (Heimgartner, 2014). One item, which is particularly vulnerable to earthquakes (Ersoy, et al., 2008), and utilities do not stock spares of due to costs, is the high voltage transformer. If the entire transformer needs to be replaced, the new one will arrive in 18-24 months post event (Berkeley & Wallace, 2010). Dr. Leon Kempner has determined the amount of damage done to high-voltage electrical substation equipment is directly related to the equipment voltage level. For instance, worldwide experience has shown 115 kV transformers and below tend to sustain slight damage, while 230 kV transformers experience moderate damage, and 500 kV transformers tend to sustain significant damage. Particularly susceptible to earthquake damage are the high voltage substation porcelain components which are a very brittle material. In addition, as noted in Table 1, when a busbar is too rigid or when there is inadequate slack available in the flexible aluminum

rope connections between substation equipment, equipment failures also result. Some actions Bonneville Power Association (BPA) has taken to mitigate the effects of undesired seismic motions are anchoring power transformers and reactors, adding supplemental structural bracing for transformer accessories, anchoring station service transformers, and restraining batteries to their racks and installing battery spacers (Knight & Kempner, 2004). However, even with these improvements, it is not guaranteed a system will come through a major seismic event without major damage.

This research focuses on determining the probability of being in a particular damage state by earthquakes of various sizes for the electrical power distribution system. This research takes several different Institute of Electrical and Electronic Engineers (IEEE) test node systems and subjects them to earthquakes of varying strengths, then creates an abstract model of the test node

system, with the probability of being within a damage state for the different areas of the system. An example of an abstract model can be seen in Figure 1.

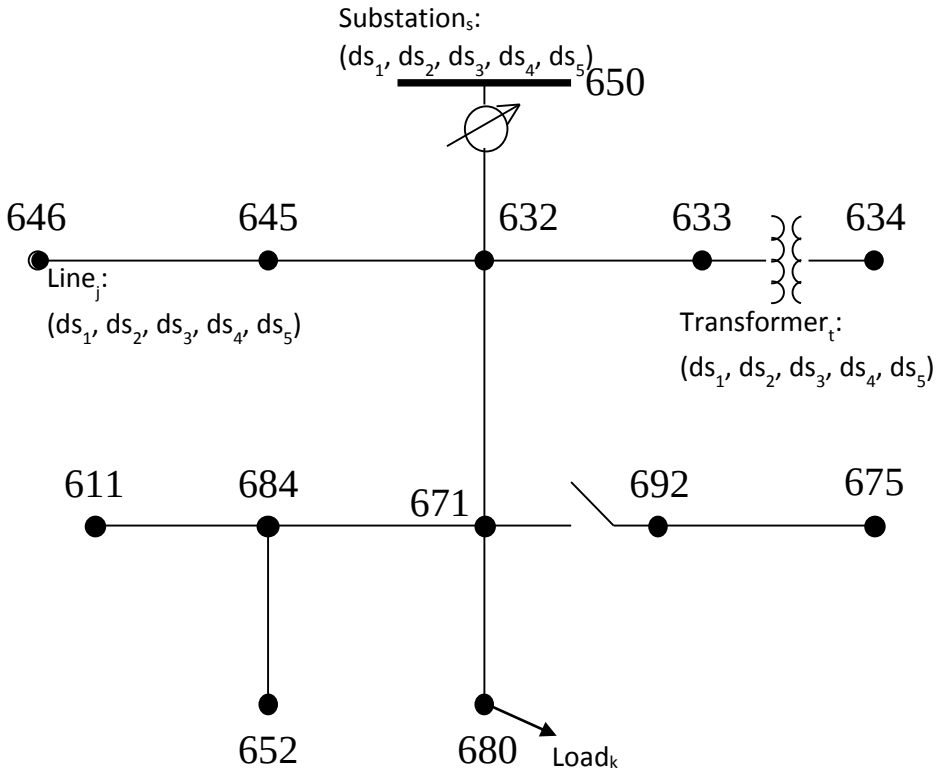

Figure 1: IEEE 13 Node Test Feeder Abstract (Distribution System Analysis Subcomittee, n.d.)

The probability a component is in a particular damage state to each component is reflected by the notation: ds_1, ds_2, ds_3, ds_4, ds_5. It is repeated for each component within the system. For clarity, it is only shown in Figure 1 for one of each of the component types. In addition, the abstract model indicates the load carried at each node. Again, for clarity, it is only indicated for one node in Figure 1.

This work varies from others by looking into damage from earthquakes, as opposed to another natural disaster such as hurricanes as is the focus of the work of Min Ouyang and Leonardo Dueñas-Osorio. In addition, this research looks at the system as a whole, as opposed to component by component, as other research completed by MCEER has done. Also, as opposed to strictly looking at how to improve the resilience of a particular component, this work

seeks to help reduce the harm done to the population by determining how to respond more effectively post natural disaster.

This thesis will give a general overview of earthquake formation and characteristics, probabilistic seismic hazard analysis (PSHA), required, or design, response spectrum, and performance based seismic design. PSHA is used to determine the potential impacts of an earthquake on a given location. Required response spectra provide seismic design criteria for structures. Performance based seismic design evaluates how a given structure will react to a seismic even through fragility curves. Fragility curves are used by the American Society of Civil Engineers (ASCE) and IEEE to determine the probabilistic damage state equipment may be in post natural disaster.

2.1. Earthquakes: An Overview

According to widely accepted theory, the earth is composed of 15 to 20 tectonic plates, which float over the earth's heated mantle. Figure 2 shows how the plates lie on the earth's mantle (Pacific Northwest Seismic Network, n.d.). Where the plates touch, also called a plate boundary, interactions occur (Fichter & Baedke, 2000). These boundaries are also known as faults.

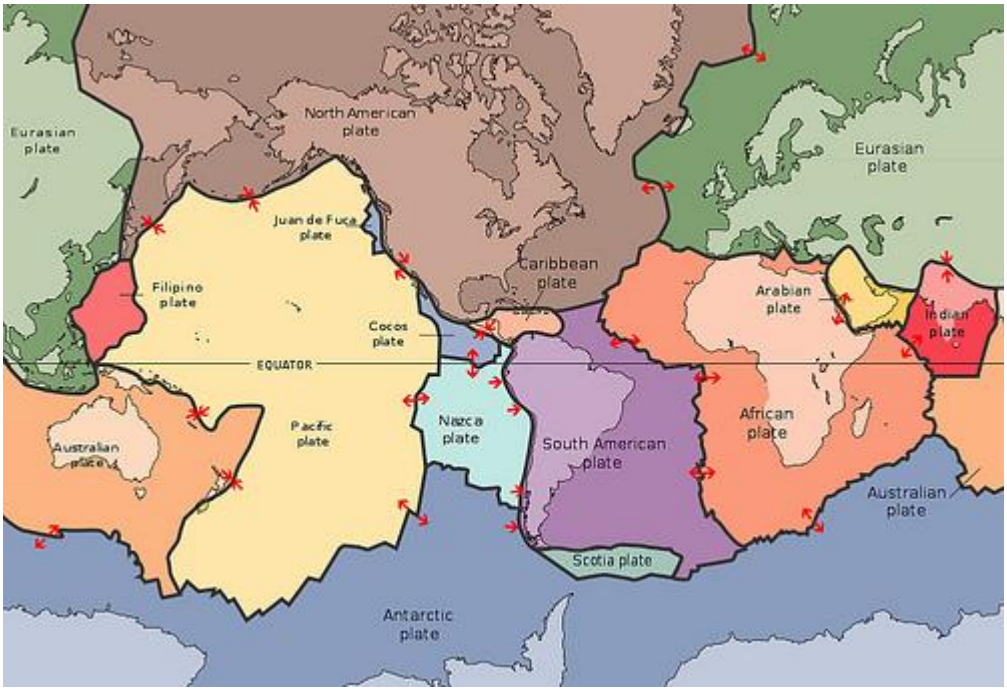

Figure 2: A depiction of the 15 to 20 tectonic plates which make up the Earth's crust (Pacific Northwest Seismic Network, n.d.).

Figure 3 shows a depiction of the three different types of boundaries formed: divergent, convergent, and transform. The interactions of the plates at these boundaries results in earthquakes with varying characteristics.

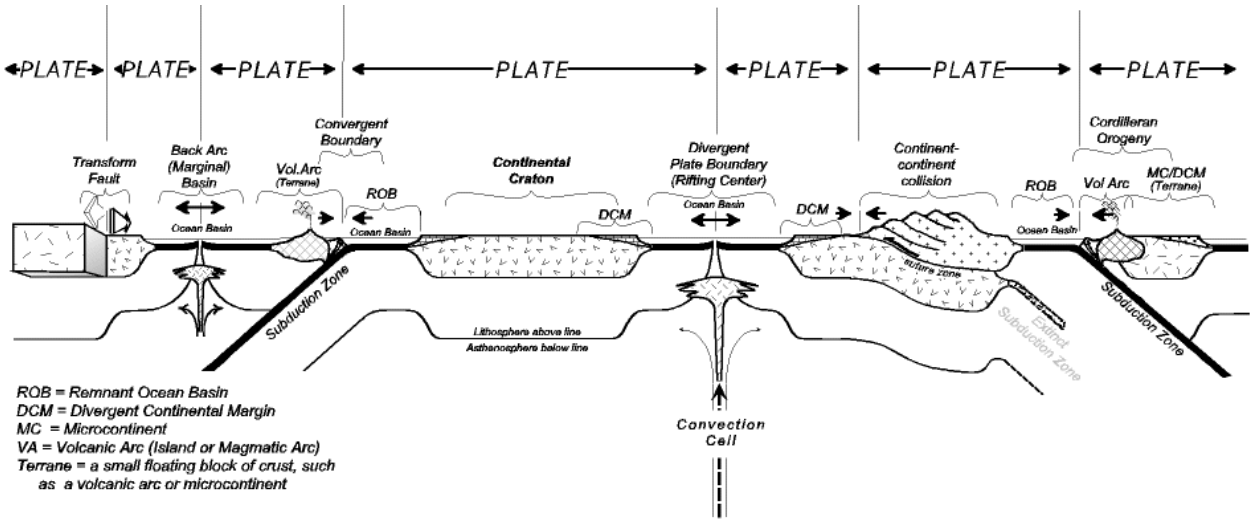

Figure 3: A depiction of the different types of plate interactions (Fichter & Baedke, 2000).

Divergent boundaries occur where two plates are separating. These types of boundaries always create a new ocean floor. Examples of divergent boundaries are found in Figure 3 on the far right and left hand sides of the figure. Convergent boundaries involve subduction zones (Fichter & Baedke, 2000). A subduction zone occurs where one plate is sliding under another. As the subducting plate is pushed further and further into the earth's mantle, it eventually breaks off, causing the remaining part of the plate to "spring" up, much as a springboard moves upward after a diver bounces off the end. When the plate "springs" back, an earthquake occurs. The larger the upward motion of the plate, or conversely, the heavier the piece of the plate which broke off, the larger the earthquake. This is the type of earthquake which occurs in the Pacific Northwest, where the Juan de Fuca plate is subducting beneath the North American plate. Figure 4 illustrates how the Juan de Fuca plate is moving beneath the North American plate. This is one of the faults having the potential to release enough energy to cause a Richter scale Magnitude 9 earthquake (Pacific Northwest Seismic Network, n.d.).

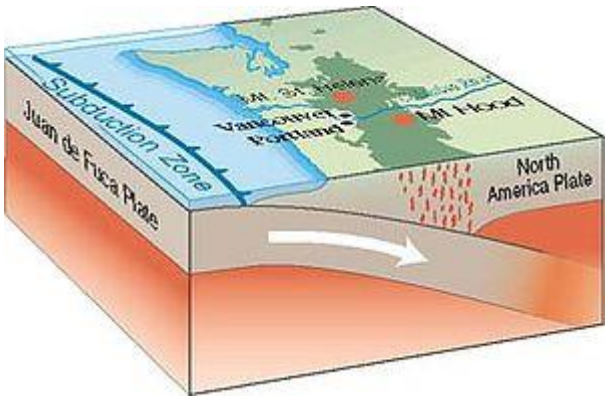

Figure 4: The Juan de Fuca plate subduction zone (Wikipedia, n.d.)

When the plate boundaries are examined closely, microplates are revealed at the boundaries of the plates. Again, the boundaries between microplates can be called faults, and when the microplates move against each other, an earthquake occurs (Berman, 2014). This helps

to explain the multitude of faults, and therefore the numerous locations of earthquakes, even when there is no interaction between two major tectonic plates (Pacific Northwest Seismic Network, n.d.). Figure 5 shows some of the faults encountered in Northwestern Oregon, caused by movement between microplates.

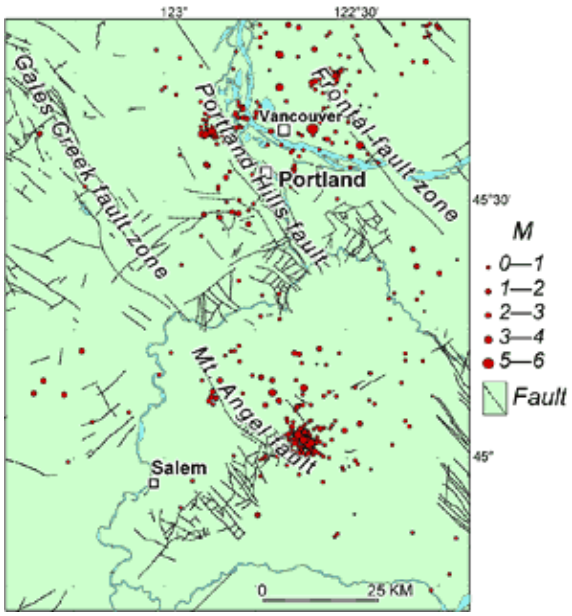

Figure 5: A depiction of various faults in Northwestern Oregon (U.S. Department of the Interior, 2012).

The final type of boundary, the transform boundary, found on the extreme left side of Figure 3, is formed by two plates moving past each other horizontally. This movement occurs relatively quietly. Most faults of this type are found in ocean basins, however, the San Andreas Fault in California and Mexico is a land example (Fichter & Baedke, 2000).

Once the movement of two plates against each other at a fault point overcomes the delicate balance between the two, an earthquake occurs. There are two ways an earthquake

relieves the pressure, either through a dip slip movement or a strike slip movement. Figure 6 shows how the land responds to each of these types of earthquake movements (Berman, 2014).

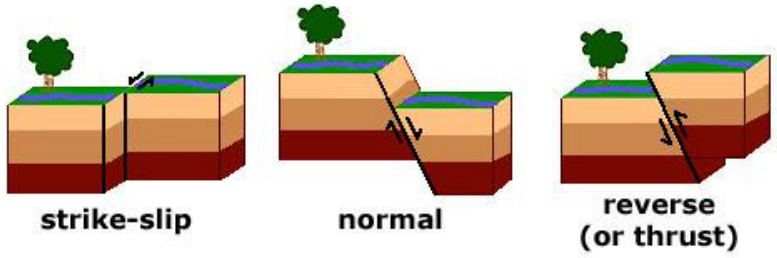

Figure 6: Far left: a normal dip slip movement, Middle: a thrust dip slip movement, Far right: a strike-slip movement (Anon., 2006).

A normal fault, where the hanging wall drops, as shown in the far left image in Figure 6, occurs due to tensile stresses in the crust. A reverse fault, where the hanging wall climbs, occur due to compressive stresses in the crust. A thrust fault is a reverse fault with a shallow dip angle. The middle picture in Figure 6 shows a thrust fault. A strike-slip movement occurs when the earth moves laterally against itself, as shown in the far right image of Figure 6 (Berman, 2014). No matter what type of movement is caused by the earthquake, all fault ruptures, or earthquakes, release vibrations, radiating outward in the form of seismic energy. These seismic energy waves are what cause infrastructure damage during an earthquake due to their frequency and how they cause the ground to move.

Having discussed how and why earthquakes occur, a look at Probabilistic Seismic Hazard Analysis (PSHA) is now needed.

2.2. Probabilistic Seismic Hazard Analysis

Unfortunately, like all other natural disasters, where and when an earthquake is going to occur next is difficult to determine. Not all of the earth's faults are known, and even when a fault location has been identified, it is difficult to determine precisely how the ground will

continue to shift and move or how it will release its next wave of seismic energy. Instead, engineers and scientists use PSHA in order to determine a location's susceptibility to an earthquake's motion. They begin by researching and understanding the seismic faults which can affect a given location. Once a site and a fault have been chosen for scrutiny, one of the ground motion parameters must be chosen as a performance factor. These ground motions include: amplitude, frequency, and duration. Amplitude parameters are peak accelerations, which can occur in either the horizontal, known as peak horizontal acceleration (PHA) or peak ground acceleration (PGA), or the vertical, known as peak vertical acceleration, directions. This parameter is useful for analysis due to the relationship which exists between the peak accelerations and inertial forces. When using this parameter, however, other parameters may also be necessary to characterize the ground motion because a large PHA with high frequencies does not necessarily result in a very damaging earthquake. Peak horizontal velocity may be a better parameter to describe ground motion as it is less sensitive to high frequencies. The final amplitude parameter which can be used for analysis is peak displacement. Peak displacement is typically associated with the low frequency components of earthquake motion. Unfortunately, peak displacement is difficult to calculate due to interference from low frequency noise. Frequency can also be used as a ground motion parameter for analysis. The response of physical systems is very dependent upon the earthquake's frequency. Each earthquake is unique, with its own frequency and acceleration spectra. If the earthquake frequency is too close to a given structure's natural frequency, resonance occurs and the structure responds in an unbounded fashion, potentially resulting in unanticipated damage. In addition, an earthquake is not limited to one specific frequency. Rather, ground motions contain components that span a broad range of frequencies. Frequencies are used in determining the desired response spectra of a system.

Response spectra will be addressed later in this section. Finally, duration can be used to describe the earthquake. In general, the longer a seismic event lasts, the more damage is done. However, duration damage also depends on frequency. A long duration, low amplitude seismic event may cause more damage than a high amplitude short duration seismic event due to the number of load reversals which have occurred in the structure over the course of the seismic event. In addition, duration is highly dependent upon local soil conditions. Different structures may experience different duration lengths for the same event due to the soil upon which the structure is built (Berman, 2014).

Once a ground motion parameter has been chosen, many different scenarios must be considered. Earthquakes cannot be predicted accurately due to the number of unconstrained variables which must be considered. Figure 7 illustrates the issue of directivity. Directivity is defined as "the preferential direction of propagation of the seismic energy emitted by a source." (Lavergne, 1989) Because the direction of propagation of a seismic event is unknown until the event is complete, engineers and scientists must run multiple scenarios simulating multiple propagation signals. In Figure 7, site A and site B see different signals due to soil conditions and wave propagation properties for a given seismic event.

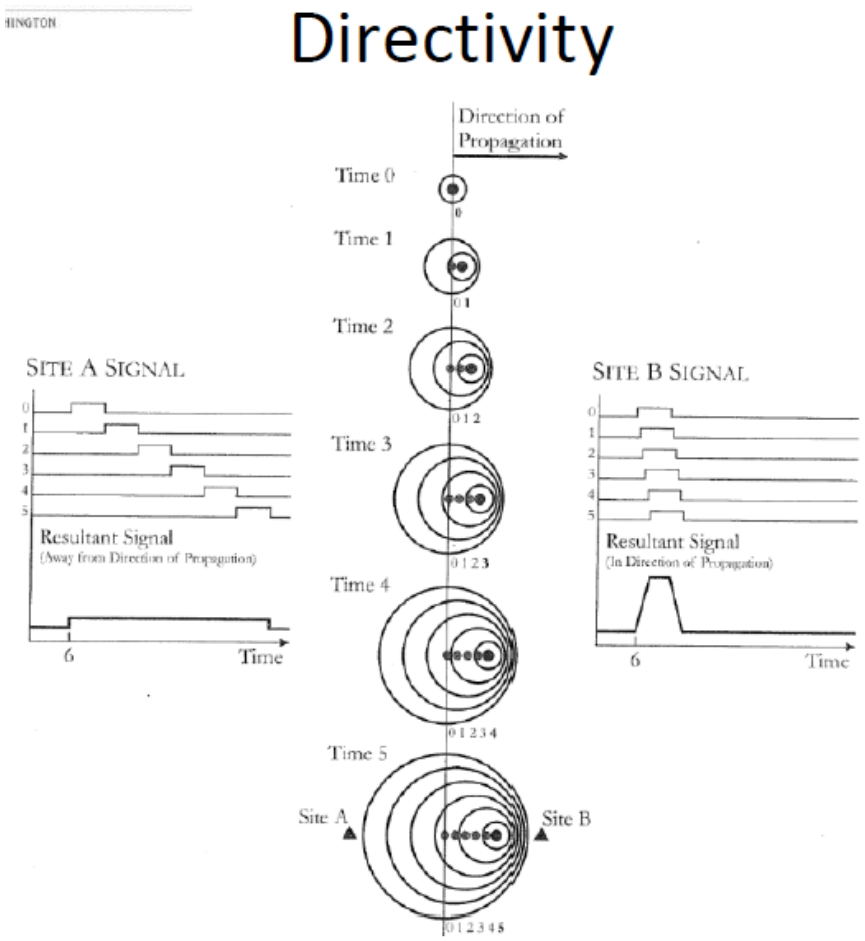

Figure 7: Illustration showing how directivity principles affect the seismic signals a structure is exposed to (Berman, 2014)

Important ground motion parameters must be estimated in order to achieve proper characterization of earthquakes for the design of infrastructure systems. The two largest influencing factors are the magnitude of the seismic waves and the distance from the source to the site: both the epicentral (R2) and hypocentral (R1) distances as well as the closest distances to high-stress zones (R3), fault rupture surfaces (R4), and the surface projection of the rupture (R5). These relationships can be seen in Figure 8.

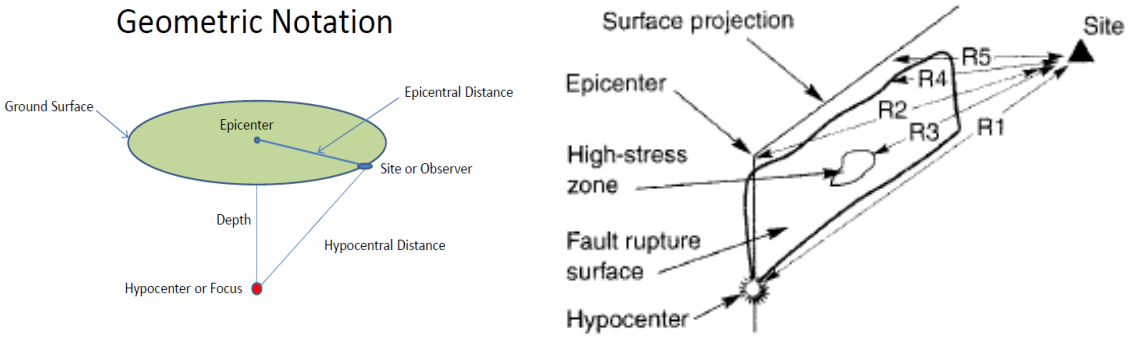

Figure 8: Geometrical relationships between the seismic rupture site and the affected site (Berman, 2014).

These geometric relationships allow the engineer to express a ground motion parameter in terms of the moment magnitude of the seismic event, the distance between the source and the site of interest, and other variables, which, if necessary, will be determined by the assessing engineer. The moment magnitude is a function of the seismic moment and is a measurement of the earthquake intensity. An attenuation relationship, a predictive relationship for parameters which decrease with increasing distance such as PGA, can then be established using existing ground motion data. These relations do have a degree of uncertainty in them, resulting in the application of standard deviation for analysis purposes (Berman, 2014).

Once identification and characterization has been attained as described above, the temporal distribution, or the recurrence relationship for a given location, must be characterized. The recurrence relationship describes the average rate at which an earthquake of some size will be exceeded. This relationship is determined for each source zone. The key assumption for determining the recurrence relationship of a given site is that past seismicity is an appropriate prediction of future seismic activity. In some parts of the world, written seismic records date back as far as 3000 years, however, in other areas, such records only exist for the past 300 years. What has been seen through these records, is that a given source can produce different magnitude earthquakes. The larger the earthquake magnitude, the less often it occurs. The opposite is also

true, in that a given source will produce low magnitude earthquakes more often on a geologic time scale (Berman, 2014). In the 1930's, Beno Gutenberg and Charles Richter, two pioneers of modern seismology, described a pattern relating the number of earthquakes in a given area over a fixed period of time to the magnitude of the earthquakes. This relationship is called the Gutenberg-Richter relationship (Southern California Earthquake Data Center, n.d.). It calculates the mean annual rate of exceedance, λ_M, or the average number of earthquakes calculated to exceed a given magnitude in any given year. It is obtained by dividing the number of exceedances, N_M, by the length of time period in records, T. The calculated return period, T_R, of a given earthquake of a given strength is the inverse of λ_M. When plotted on a lognormal plot, the relationship is linear, as illustrated in Figure 9.

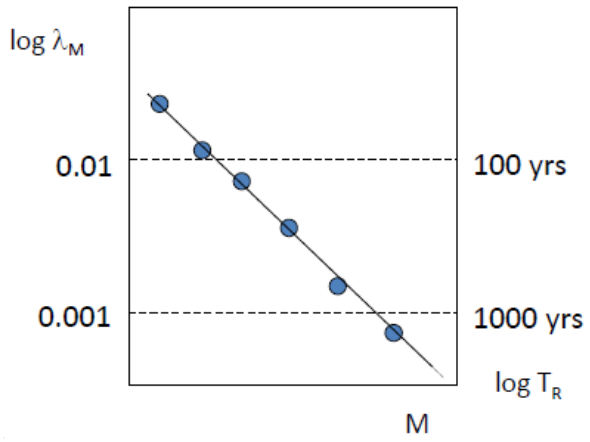

Figure 9: Illustration of the mean annual rate of exceedance and the return period of an earthquake of magnitude M (Berman, 2014).

The linear relationship between magnitude and the annual rate of exceedance is then summarized by the Gutenberg-Richter Recurrence Law, in Equation (2.1).

$$\log \lambda_M = a - bM \tag{2.1}$$

Where:

λ_M = the mean annual rate of exceedance

a = the y intercept

b = the slope of the line

M = the magnitude of the earthquake

For the purposes of this research, this relationship is sufficient. It must be noted, however, that this relationship does not take into account the limitations of the magnitudes of earthquakes (Berman, 2014). The strongest earthquake recorded is a 9.5 magnitude earthquake which occurred in Chile on May 22, 1960. There are no faults on earth capable of producing a 10.5 magnitude earthquake (U. S. Department of the Interior, 2014). This relationship is bounded for each fault because each fault can only produce up to a certain strength earthquake due to its size, length, and depth (Berman, 2014).

The Gutenberg-Richter relationship helps explain how often earthquakes of a certain size occur. What is now needed is how to determine the probability of a certain sized earthquake occurring in a given year. To do this, a Poisson distribution, a random distribution, is used. This distribution has no memory, meaning that the number of occurrences in one time interval is independent of the number which occur in any other interval. The probability of occurrence during a very short interval is proportional to the length of the interval, and the probability of more than one occurrence during a very short interval is negligible. A Poisson distribution is defined as the probability of a random variable, N, representing the number of occurrences of an event in a given time interval. This is show in Equation (2.2).

$$P[N = n] = \frac{\mu^n - e^{-\mu}}{n!} \tag{2.2}$$

Where:

N = number of occurrences in a given time interval

μ = the average number of occurrences in the given time interval

For PSHA usage, the temporal distribution of earthquake recurrence is given by Equation (2.3)

$$P[N = n] = \frac{(\lambda t)^n e^{-\lambda t}}{n!} \tag{2.3}$$

Where:

λ = the average rate of occurrence

t = the time period of interest

To determine the probability of a single occurrence, Equation (2.4) is used.

$$P[N \geq 1] = 1 - e^{-\lambda_m t} \tag{2.4}$$

Equation (2.4) is then used to determine the 2% exceedance in 50 years, also known as the maximum considered earthquake (MCE) for a given fault. Current code requires all structures be designed to withstand a 2/3 MCE earthquake for the fault under consideration (Berman, 2014).

There are numerous uncertainties which must be accounted for using PSHA. The first is the location, modeled as the source to site distance probability distribution function. Second is the size of the earthquake, modeled as the magnitude probability distribution function; third is the predicted effects of the earthquake, modeled with the attenuation relationship including standard error. Finally, there is uncertainty in the timing of the earthquake, modeled using the Poisson model. All of the calculated probabilities and uncertainties are then combined together using the Total Probability Theorem, defined in Equation (2.5).

$$P[A] = P[A \mid B_1]P(B_1) + P[A \mid B_2]P(B_2) + ... + P[A \mid B_N]P(B_N) \tag{2.5}$$

To relate the Total Probability Theorem directly to PSHA, Equation (2.6) is used.

$$P[Y > y^*] = \iint P[Y > y^* \mid m, r] f_M(m) f_R(r) dm dr \quad (2.6)$$

Where:

Y = the ground motion parameter of interest

y^* = the exceedance parameter of Y

$f_M(m)$ = the magnitude probability distribution function

m = the magnitude of the earthquake

$f_R(r)$ = the source-site distance probability distribution function

r = the distance from the epicenter of the earthquake

Equation (2.6)gives the probability that y^* will be exceeded if an earthquake occurs. To calculate the annual rate of exceedance, the probability of exceedance, found in Equation (2.6), is multiplied by the annual rate of occurrence of earthquakes. In reality, most sites are affected by more than one source. In addition, most probability distribution functions for the magnitudes and distances are too complicated to integrate analytically, so the problem is solved numerically. This can be seen in Equation (2.7) (Berman, 2014).

$$\lambda_{y^*} = \sum_{i=1}^{N_S} \sum_{j=1}^{N_M} \sum_{k=1}^{N_R} v_i P[Y > y^* \mid m_j, r_k] P[M = m_j] P[R = r_k] \quad (2.7)$$

Where:

λ_{y^*} = the annual probability a ground motion parameter exceeds a ground motion parameter of interest

N_S = all sites

N_M = all possible magnitudes

N_R = all possible distances

$P[Y > y^* | m_j, r_k]$ = possible effects, weighted by its conditional probability of occurrence

$P[M = m_j]$ = the contribution of a magnitude weighted by its probability of occurrence

$P[R = r_k]$ = the contribution of a distanced weighted by its probability of occurrence

The end result is the plot shown in Figure 10, the seismic hazard curve. It shows the mean annual rate of exceedance of a particular ground motion parameter. This is the ultimate result of PSHA (Berman, 2014).

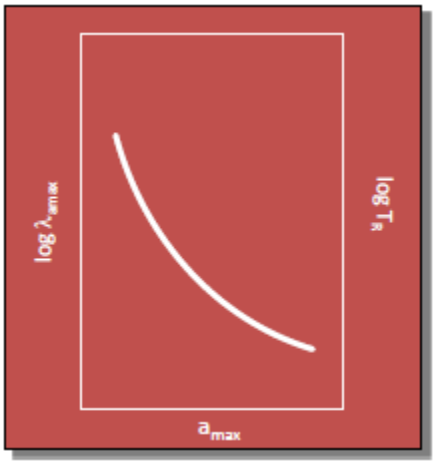

Figure 10: A seismic hazard curve, the ultimate result of a PSHA (Berman, 2014).

2.3. Required (Design) Response Spectrum

Once scientists and engineers have determined the MCE for a given site, a structure is designed following ASCE and IEEE guidelines. These guidelines look at the first mode response of an event which has a 2% chance of exceeding the seismic hazard level in 50 years, or the MCE. The structure is designed for an earthquake of strength 2/3 MCE (Berman, 2014). Two documents which help guide engineers in designing structures to meet this demand are ASCE 7, for buildings, and IEEE 693 for electrical substations. IEEE 693 is a voluntary standard, applies to new construction, not retrofit design, and does not have to be followed by any utility which is building a new substation. However, in the interest of protecting their investments, most utilities, particularly those in seismically active locations, choose to follow it. It pertains to the equipment used in substations, because substations, in particular substation transformers, have been shown to be the most susceptible to damage during an earthquake (Murota, et al., 2005). IEEE 693 provides the framework and procedures to test substation

equipment against seismic loads, and then compare the responses to pre-defined required response spectrum (RRS). An example RRS can be found in Figure 11. An RRS gives a maximum response allowed to for the various frequency spectra of an earthquake (IEEE Power Engineering Society, 2005). An RRS can be developed without using site-specific ground motion procedures. Because this research was done to be generic in location, this is the method which will be described (American Society of Civil Engineers, 2010). There are three different curves, corresponding to different damping levels. Electrical equipment is typically afforded minimal damping, so the 2% curve should be the one considered (Berman, 2014).

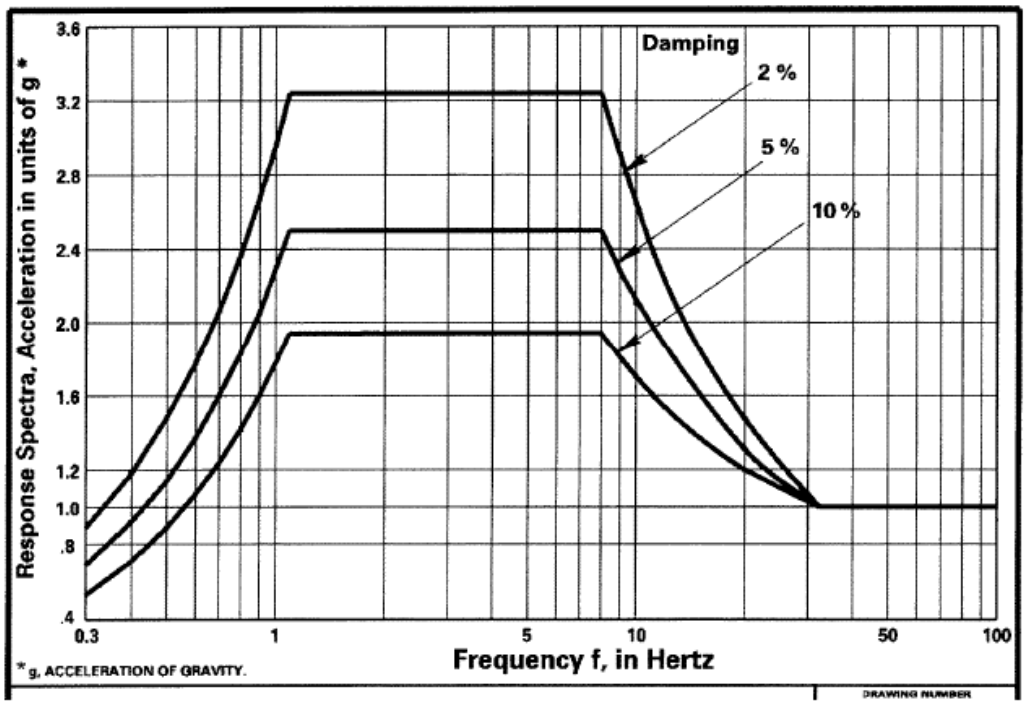

Figure 11: An example RRS plot. This plot shows the qualification standard for equipment expected to experience a high seismic level (IEEE Power Engineering Society, 2005).

An RRS is a plot of Spectral Response Acceleration, S_a in g, vs the Period, T in seconds. There are three distinct parts to an RRS. They are shown in Figure 12. Region 1 starts at $T < T_S$ and extends through $T = T_S$. It is the short period range representing constant spectral response acceleration. It consists of two lines, the first beginning at $T = 0$ and ending at $T = T_0$. The

second line begins at $T = T_0$ and ends at $T = T_S$. Region 2 begins at $T = T_S$ and ends at $T = T_L$. It is the long period range representing constant spectral response velocity. Region 3 begins at $T = T_L$. It is the very long period range representing constant spectral response displacement. Region 3 is only considered for very tall buildings (>30+ stories). Region 3 is not relevant to this research (American Society of Civil Engineers, 2010).

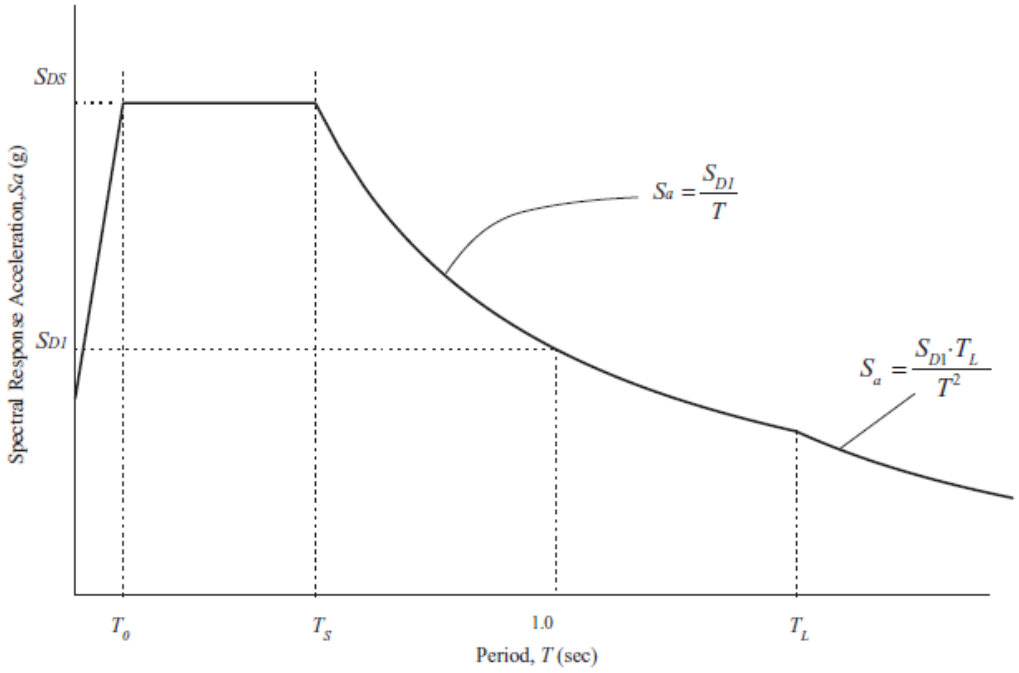

Figure 12: A depiction of how to determine the different parts of a required response spectrum (American Society of Civil Engineers, 2010).

The equations for the lines are given by Equation (2.8) – Equation (2.11).

$$S_a = S_{DS}(0.4 + 0.6\frac{T}{T_0}) \tag{2.8}$$

$$S_a = S_{DS} \tag{2.9}$$

$$S_a = \frac{S_{D1}}{T} \tag{2.10}$$

$$S_a = \frac{S_{D1} T_L}{T^2} \tag{2.11}$$

Where:

S_a = the spectral response acceleration

S_{DS} = the design spectral response acceleration parameter at short periods

S_{D1} = the design spectral response acceleration parameter at 1-s period

T = the fundamental period of the structure

$$T_0 = 0.2 \frac{S_{D1}}{S_{DS}}$$

$$T_S = \frac{S_{D1}}{S_{DS}}$$

These parameters are fully explained in ASCE 7.

MCEER has qualified electrical equipment utilizing IEEE 693, and experimented with different ways of anchoring and mounting components in order to increase equipment robustness. Descriptions and results of these experiments can be found in two technical reports, MCEER 05-0008 and MCEER 08-0011. Qualifying equipment and anchorage systems as defined in IEEE 693 provides resiliency and robustness to the electrical system.

These two concepts, PSHA and RRS, provide design requirements for engineers. These requirements help make a strong and robust system. However, because the designs are based off of probabilistic scenarios, damage can still occur to a system. The probability of the extent of damage to be incurred can be modeled using fragility curves.

2.4. Performance Based Seismic Design

The goal of using Performance Based Seismic Design is to ensure structures and facilities are earthquake resistant. Performance Based Seismic Design is utilized in terms of structural capability; it does not consider how internal mechanical and electrical systems will respond to an earthquake. This means that even if a building is structurally sound after an earthquake, the building may still be abandoned or torn down by its owners due to interior issues (Berman, 2014). With regards to the electrical distribution system and its associated buildings, this stipulation is not usually an issue due to the intended use and occupancy of the structure. Performance Based Seismic Design creates and utilizes fragility curves to estimate the probabilistic future seismic performance of structures in terms of system level decision variables.

2.4.1. Fragility Curves

Fragility curves are made to help explain to business owners, government officials, and those with assets vulnerable to earthquakes what costs and benefits can be seen with upgrades and improvements to their buildings. The decision variables used to create fragility curves are performance measurements which are meaningful to the general public, such as repair cost, casualties, and loss of use – either dollars, deaths or downtime. The complete methodology in fragility curve use involves four stages: hazard analysis, structural analysis, damage analysis, and loss analysis (Porter, et al., 2007). This research stops at the third stage: damage analysis, in reference to the electrical distribution system.

At its core, a fragility curve is a cumulative probability distribution function. It is composed of three different models: the response model, the damage model, and the loss model. It has three inputs and one final output. The inputs are: ground motion, system response, and physical damage, with the output being expected losses. A flowchart is shown in Figure 13

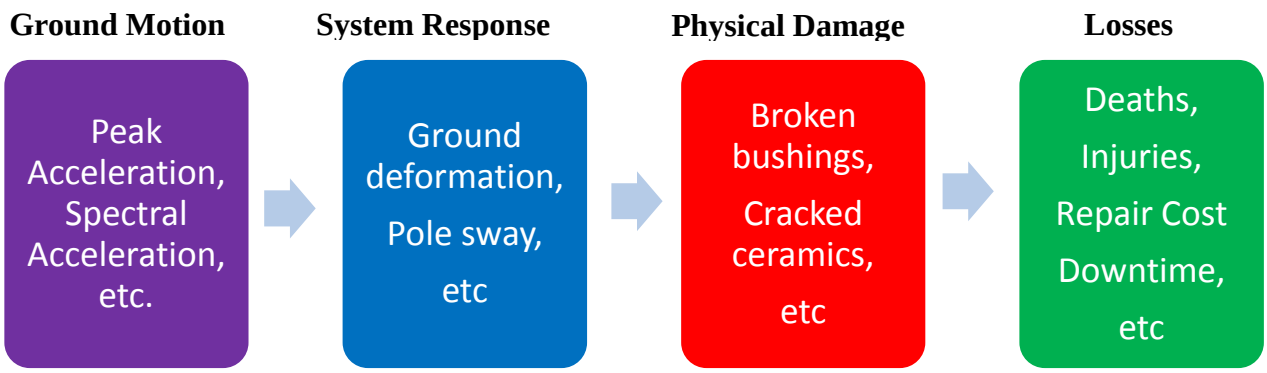

Figure 13: Fragility curve creation flowchart

All of these inputs are uncertain. Current technology does not allow accurate estimation of the size or strength of the next earthquake. Because the ground motion reaching the structure is unknown, the exact system response is unknown. With the system response unknown, it is unknown how much physical damage will occur, and how much loss will be incurred. This process must also take into account every ground motion parameter, not just one, which ultimately affects the predicted loss outcome (Berman, 2014).

As stated previously, a fragility function is a cumulative distribution function, depicted using a lognormal scale. The loss function fragility curve is described by Equation (2.12). It is made up of three other fragility curves.

$$\lambda(DV) = \iiint G(DV \mid DM) \mid dG(DM \mid EDP) \mid\mid dG(EDP \mid IM) \mid\mid d\lambda(IM) \mid \qquad (2.12)$$

Where:

$\lambda(DV)$ = the loss function

DV = the Decision Variable

DM = the Damage Measure

EDP = the Engineering Demand Parameter

IM = the Intensity Measure

The first fragility function calculated in this loss function is the response given the ground motion. It describes the probability of exceeding a certain *EDP* with a given *IM*. This results in multiple curves, each corresponding with a different *EDP*. The next fragility curve calculated the damage given the response. It is the probability of damage for a given *EDP*. The final fragility curve is that of loss given the damage. It is the probability of a cost to repair the damage given a damage level. These three fragility curves are then integrated together to determine the loss function in terms of annual probable loss. An example can be seen in Figure 14. This curve shows two different annual probabilities of loss and their expected cost in dollars (Berman, 2014).

Figure 14: Example loss fragility curve, calculated in terms of cost (Berman, 2014).

This research utilizes the first two fragility curves. The purpose of this research was to determine the expected damage after an earthquake with respect to the electrical distribution system. It is possible to calculate the damage given ground motion, which is what was done for this research (Berman, 2014).

Two equations were used to create the fragility models for this research. They are listed as Equation (2.13) and Equation (2.14).

$$F_{dm}(edp) \equiv P[DM \geq dm \mid EDP = edp] \tag{2.13}$$

Where $F_{dm}(edp)$ is the fragility function for the damage state *dm*, which is defined as the probability a component reaches or exceeds the damage state *dm* for a particular, given *EDP* value. Equation (2.13) is then idealized by a lognormal distribution, as shown in Equation (2.14).

$$F_{dm}(edp) = \Phi\left(\frac{\ln(\frac{edp}{x_m})}{\beta}\right) \tag{2.14}$$

Where:

Φ = standard normal cumulative distribution function

x_m = the median value of the distribution

β = the logarithmic standard deviation

The fragility function as shown in Equation (2.14)can be seen graphically for the distribution circuit with seismic components in Figure 15.

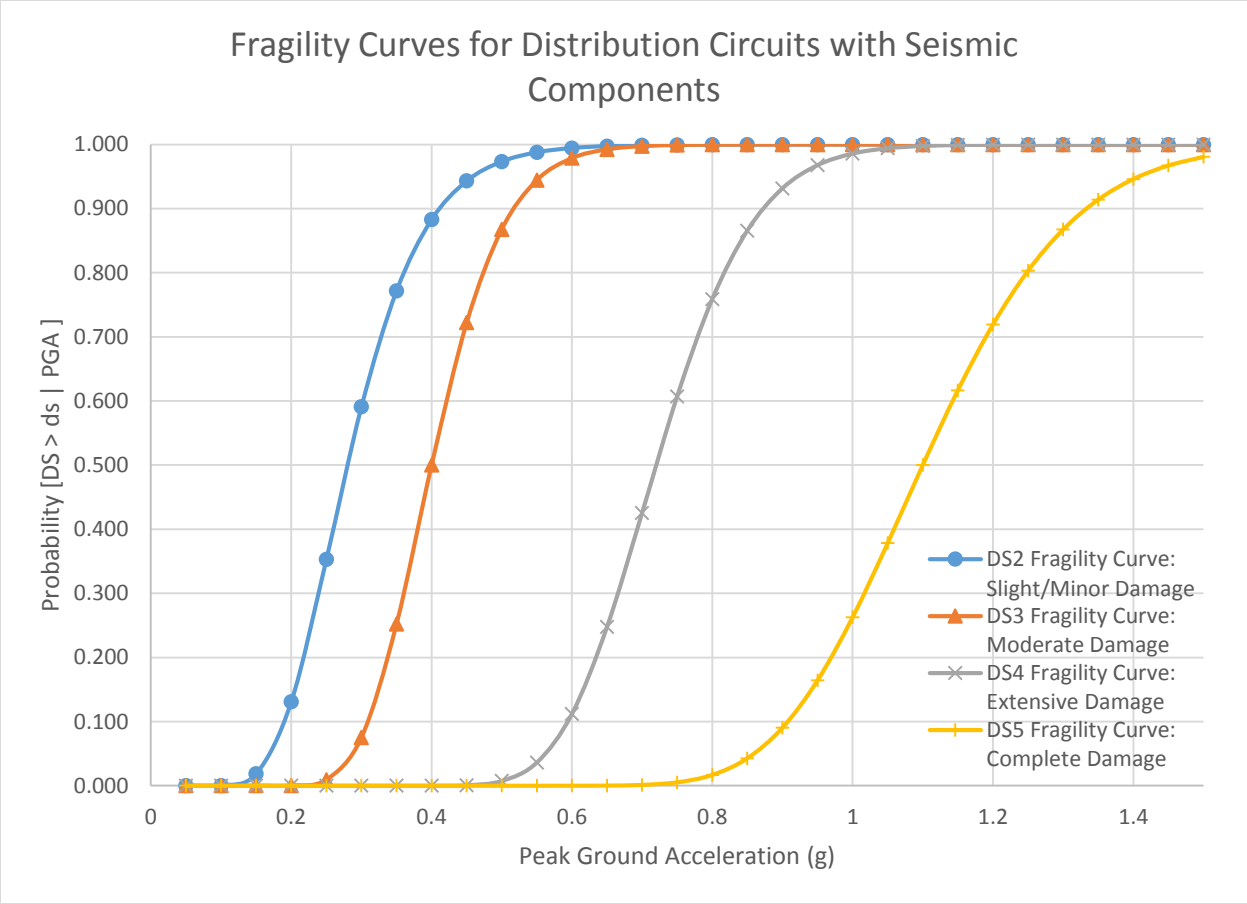

Figure 15: Fragility Curves for Distribution Circuits with Seismic Components

There are five methods which can be used to determine x_m and β, each with its own strengths and limitations. The first is the Actual *EDP*. This is the most informative way of creating a fragility function. It is used where the *DM* is associated with a point on the observed force-deformation behavior of a component. The second method is called the Bounding *EDP*, where the data includes the maximum *EDP* which each of the specimens was subjected, and whether the specimen exceeded the damage state of interest. The third method is called the Capable *EDP*, where cases have no observations of $DM \geq dm$ and a number of observations of no damage occurrences of $DM \geq dm$. The fourth method, the Derived Fragility Function method, is done by modeling the component as a structural system, and determining the *EDP* which would cause the system to reach *dm*. The fifth method, Expert Opinion, selects experts with

professional experience in the design or post-earthquake observation of the component (Porter, et al., 2007).

In order to determine the probability a component is in a certain damage state, *dm*, given *EDP* = *edp* is given by Equation (2.15) – Equation (2.17).

$$P[DM = dm \mid EDP = edp] = 1 - F_1(edp) \qquad dm = 0 \tag{2.15}$$

$$P[DM = dm \mid EDP = edp] = F_{dm}(edp) - F_{dm+1}(edp) \qquad 1 \leq dm \leq N \tag{2.16}$$

$$P[DM = dm \mid EDP = edp] = F_{dm}(edp) \tag{2.17}$$

Where:

N = the number of damage states

dm = 0 = indicates the undamaged state

An example of how the probability of a component being in a given damage state changes withrespect to PGA is shown in Figure 16.

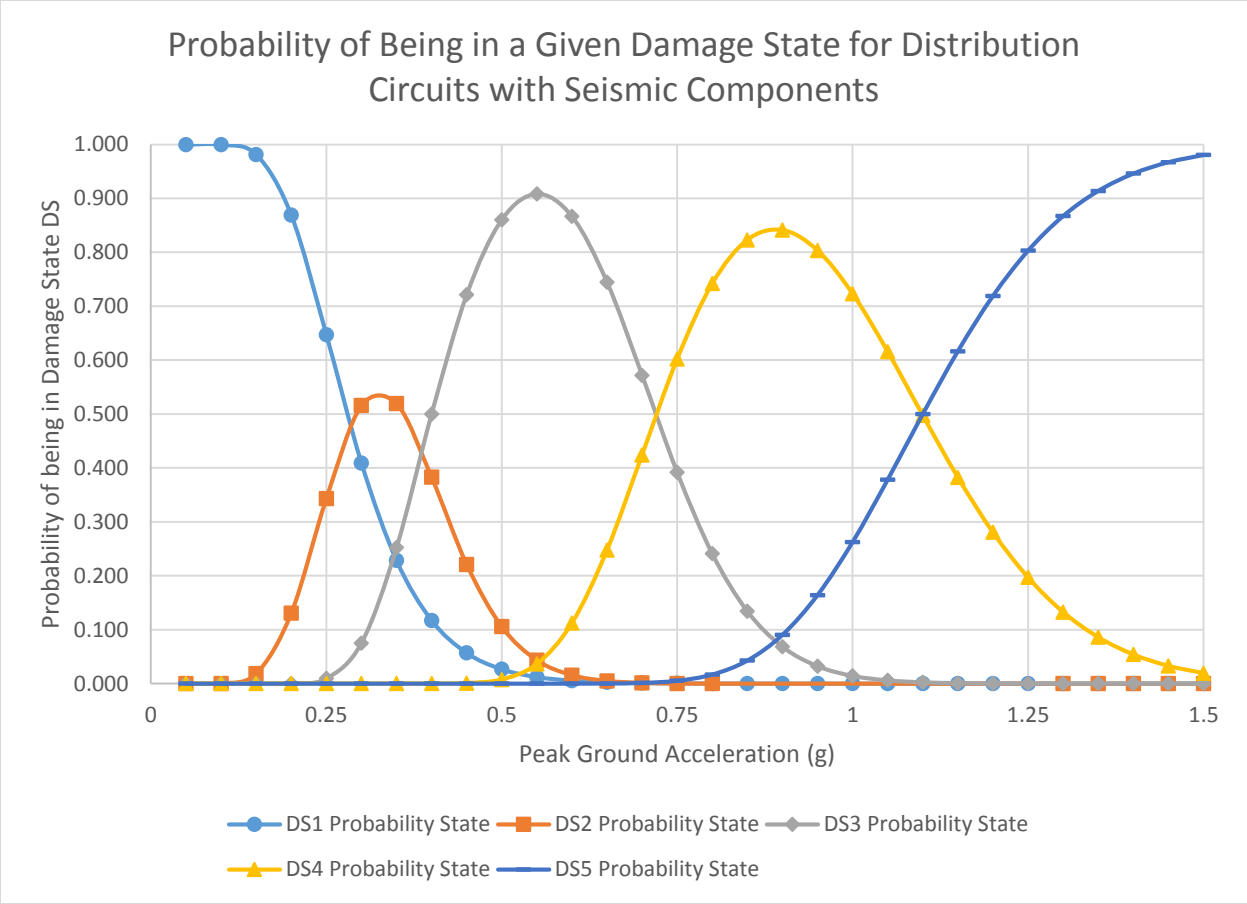

Figure 16: How the probability of a component being in a given damage state changes with respect to PGA

Understanding how to both build and interpret fragility curves is critical in attempting to predict how each part of the electrical power system will be affected (Porter, et al., 2007). This understanding helped build the required fragility curves in order to determine the probability of being in a given damage state for the electrical distribution system following an earthquake.

3. Methodology

This research ultimately created an abstract model of the electrical distribution system, linking probability of the system being in a damage state post-earthquake to lines and nodes given an earthquake PGA. This data will then be read into an optimization program to determine the optimal repair procedures given the estimated damage states and available assets. The one line diagram, showing how the system is set up for the example shown in this methodology section is shown in Figure 17. It is similar to the abstract shown in Figure 1, however, the voltage regulator between Node 650 and Node 632 has been removed. The switch between Node 671 and 692 has been replaced with a transformer, and a second substation, Node 700, has been added, connected at Node 692.

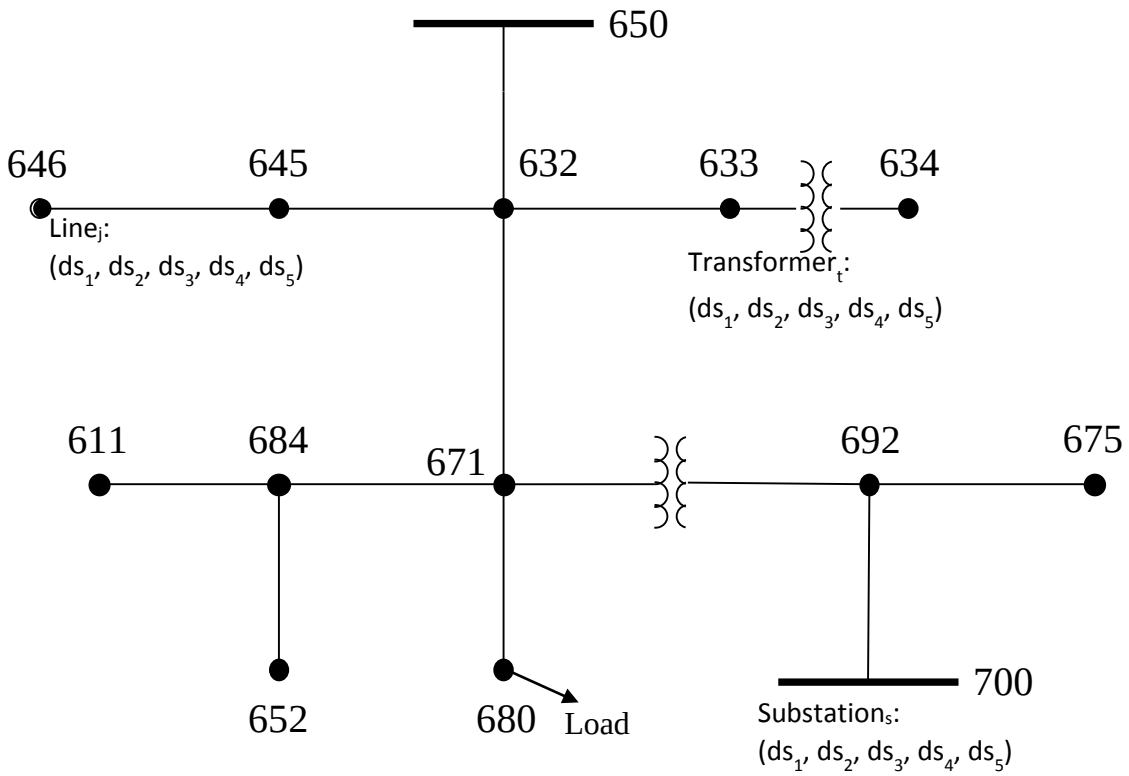

Figure 17: Example Distribution System Abstract (Distribution System Analysis Subcomittee, n.d.)

The fragility curves are used to determine the probability of being in a certain damage state given a PGA input. Each damage state has a certain amount of system damage associated with it. The

probable location of this system damage is determined in the optimization algorithm. Each line, transformer, and substation, depicted by the thick black lines, has a probability of damage state associated with it for a given PGA. These values, with their associated probability of damage state location, and the associated load values, are then fed into the optimization program to determine the fastest way to restore power to all nodes while maintaining system integrity. Figure 17 shows an entirely radial system. Many distribution systems also have switches allowing the utility to create loops within the distribution, or an alternate power path. For a system of this type, the optimization algorithm can come up with a solution on how to dispatch crews based upon predicated damage, such as shown in Figure 18. The numbers shown above the nodes are the probability of damage, based on weighted importance factors. In this case, the load amount is the determining factor for if a load is important or not. The higher the load amount, the more important the load.

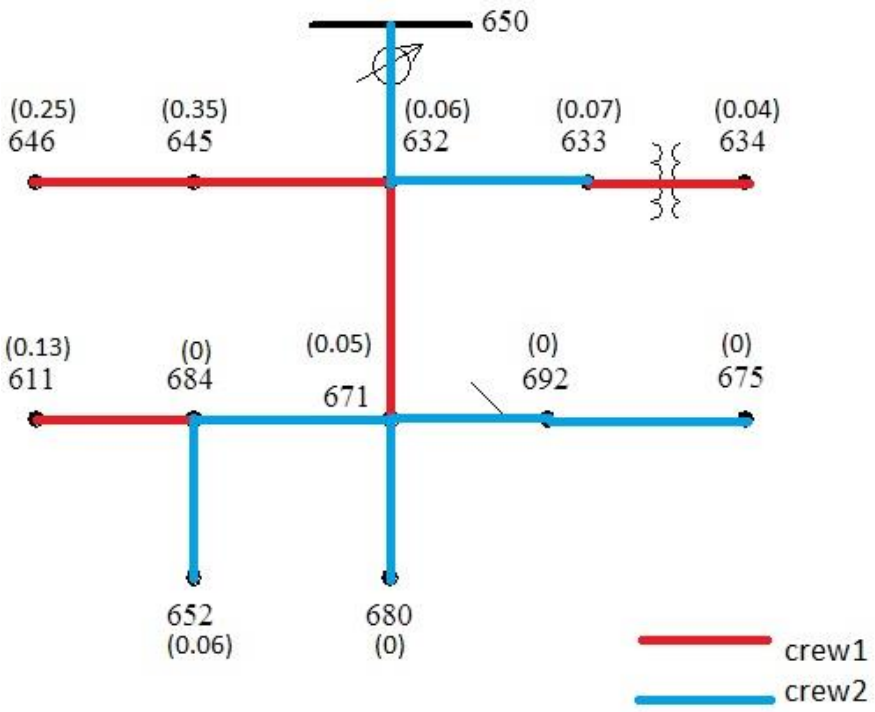

Figure 18: Potential Optimization results (Tan, 2014)

3.1. Set up

The algorithm was created using MATLAB R2014a. It reads in the system data from an Excel document. The system data used to test the algorithm are the four IEEE test systems: 13 node, 34 node, 37 node, and 123 node. However, any system can be modelled in so long as the inputs are the in the same format as the IEEE systems. This allows the user to model their system without previous knowledge of the desired simulation location or conditions. The format is shown in Table 2.

Table 2: Read in Line Segment Data format for the algorithm

Node A	Node B	Length (ft)	Config	Soil	Substation	Voltage
Node from number	Node to number	Length between nodes, in feet	Line configuration, XFM-1, or Switch	States what type of soil the component is on - ‘A’, ‘B’, ’C’,’D’,’E’	‘S’ indicates the location of a substation, otherwise, blank	Only filled in for a substation node, ‘H’,’M’,’L’

Transformers must be labeled as XFM-1, as the algorithm looks specifically for this string of characters to determine which nodes have transformers between them. Currently, switch and line configuration data is not used. The soil type must be in capital letters, as must the voltage. Soil type matters because different soil types transmit the earthquake energy waves differently. This was shown in Figure 7 and explained in the section with directivity. Physically, directivity was evidenced in the 1985 Michoacan earthquake, which had its epicenter located off the west coast of Mexico. This was a magnitude 8 earthquake along a coastal subduction zone. Some damage was experienced along the coast, however, most of the damage was located in Mexico City, 300 km away. The amount of damage done in Mexico City was due to the soil conditions of the city. Very soft clay underlies much of the city because Mexico City's location is that of an ancient lake bed. This soft clay transmits the energy waves more so than the very hard rock found in the mountains just off the coast of Mexico (Rathje, 2010). Table 3 states the different types of soils and how they are referenced as defined is ASCE 7.

Table 3: Listing of Soil Types and Descriptions

Soil Class	Soil Description
A	Hard Rock
B	Rock
C	Very dense soil and soft rock
D	Stiff soil
E	Soft clay soil

The substation column utilizes an 'S' to indicate if the node in the first column is a substation node. If the node is not a substation, nothing is written. A substation can be many different voltages, either high, medium, or low. An 'H', 'M', or 'L' in the seventh column corresponds with these voltage levels. These level indicators are only needed for those nodes which are substations. All other nodes are blank. In addition, the algorithm also reads in the system load data in the format shown in Table 4.

Table 4: Format to input Loads

Node	Load	Phase 1	Phase 1	Phase 2	Phase 2	Phase 3	Phase 3
	Model	kW	kVar	kW	kVar	kW	kVar
Node #	Y-PQ, Y-I, Y-Z, D-PQ, D-I, D-Z	Phase A real load	Phase A reactive load	Phase B real load	Phase B reactive load	Phase C real load	Phase C reactive load
	Total	Sum of Phase A real loads at all nodes	Sum of Phase A reactive loads at all nodes	Sum of Phase B real loads at all nodes	Sum of Phase B reactive loads at all nodes	Sum of Phase C real loads at all nodes	Sum of Phase C reactive loads at all nodes

The algorithm also creates a vector of PGA's, ranging from 0.05, an extremely minor earthquake, to 1.5, a major earthquake. The user is then prompted to input the desired PGA to simulate. Based upon the indicated soil type, input from Column 5 on the Line Data Excel Worksheet, the algorithm converts the desired simulation PGA to what the various components of the system will see. This conversion is based off of the coefficients found in Table 5 and Equation (2.18). A straight line interpolation is used between listed points (American Society of Civil Engineers, 2010).

Table 5: Conversion requirements from desired simulated PGA to site specific simulated PGA

Soil Class	PGA $\leq$ 0.1	PGA = 0.2	PGA = 0.3	PGA = 0.4	PGA $\geq$ 0.5
A	0.8	0.8	0.8	0.8	0.8
B	1.0	1.0	1.0	1.0	1.0
C	1.2	1.2	1.1	1.0	1.0
D	1.6	1.4	1.2	1.1	1.0
E	2.5	1.7	1.2	0.9	0.9

(American Society of Civil Engineers, 2010)

$$PGA_M = F_{PGA} PGA \tag{2.18}$$

Where:

PGA_M = the desired simulated PGA adjusted for soil class effects

PGA = the desired simulated PGA

F_{PGA} = the site coefficient from Table 5

Fragility curves for several different components are then created. The algorithm determines which fragility curves are needed based off of the indicated components. These fragility curves are also broken up by seismic or standard anchoring. The fragility curves were built using Equation (2.14). This research used the HAZUS given x_m and β (Department of Homeland Security and Federal Emergency Management Agency, n.d.). Which fragility curve creation method used to determine these values is unknown. The algorithm then determines the damage state probabilities for the various components using the relationships defined in Equation (2.15)– Equation (2.17). For this algorithm, there are five damage states, therefore N=5. The damage states are defined in Table 6. The probability of being in the damage state is outputted, not the amount of damage done to the system. The components for which fragility curves are determined and their corresponding x_m and β values are stated in Table 7 - Table 9.

Table 6: Definition of System Damage States

Damage State #	Damage State Name	Description of Amount of Damage Done	
		Substation	Distribution circuits
DS_1	No Damage	No damage	No damage
DS_2	Slight/Minor	Failure of 5% of disconnect switches, 5% of circuit breakers, or by the building being in a minor damage state	Failure of 4% of all circuits
DS_3	Moderate	Failure of 40% disconnect switches, 40% of circuits breakers, 40% of current transformers, or by the building being in a moderate damage state	Failure of 12% of circuits
DS_4	Extensive	Failure of 70% of disconnect switches, 70% of circuit breakers, 70% of current transformers, 70% of transformers, or by the building being in an extensive damage state	Failure of 50% of all circuits.
DS_5	Complete	Failure of all disconnect switches, all circuit breakers, all transformers or current transformers, or by the building being in the complete damage state	Failure of 80% of all circuits.

(Department of Homeland Security and Federal Emergency Management Agency, n.d.)

Table 7: Substation with Anchored or Seismic Components Fragility Curve Inputs

Component Type	Damage State	Median (x_m)	Variance (β)
Low Voltage	DS_2	0.15	0.70
	DS_3	0.29	0.55
	DS_4	0.45	0.45
	DS_5	0.90	0.45
Medium Voltage	DS_2	0.15	0.60
	DS_3	0.25	0.50
	DS_4	0.35	0.40
	DS_5	0.70	0.40
High Voltage	DS_2	0.11	0.50
	DS_3	0.15	0.45
	DS_4	0.20	0.35
	DS_5	0.47	0.40

(Department of Homeland Security and Federal Emergency Management Agency, n.d.)

Table 8: Substation with Unanchored or Standard Components Fragility Curve Inputs

Component Type	Damage State	Median (x_m)	Variance (β)
Low Voltage	DS_2	0.13	0.65
	DS_3	0.26	0.50
	DS_4	0.34	0.40
	DS_5	0.74	0.40
Medium Voltage	DS_2	0.10	0.60
	DS_3	0.20	0.50
	DS_4	0.30	0.40
	DS_5	0.50	0.40
High Voltage	DS_2	0.09	0.50
	DS_3	0.13	0.40
	DS_4	0.17	0.35
	DS_5	0.38	0.35

(Department of Homeland Security and Federal Emergency Management Agency, n.d.)

Table 9: Distribution Circuit Fragility Curve Inputs

Component Type	Damage State	Median (x_m)	Variance (β)
Seismic Components	DS_2	0.28	0.30
	DS_3	0.40	0.20
	DS_4	0.72	0.15
	DS_5	1.10	0.15
Standard Components	DS_2	0.24	0.25
	DS_3	0.33	0.20
	DS_4	0.58	0.15
	DS_5	0.89	0.15

(Department of Homeland Security and Federal Emergency Management Agency, n.d.)

While generation facilities are included in the HAZUS system, they are not part of the distribution system and were not included for this algorithm. This algorithm allows the user to define which types of components are installed in the system, either seismically anchored or standard components. Standard components are not anchored. All components within the system are anchored the same way. The model does not allow for the substation to be seismically anchored but the distribution system to be unanchored.

3.2. What it does

This algorithm outputs an abstract graph, linking nodes and lines with the probability of being in a damage state given a researcher's input PGA. This graph is output in Excel format in the following worksheets: Damage Lines, Damage Substations, Damage Transformers, Loads, and System Data. These worksheets are shown in Table 10 - Table 14.

Table 10: Damage Lines Worksheet example

Node From	Node To	DS_1	DS_2	DS_3	DS_4	DS_5
Node from #	Node to #	Probability of no damage	Probability of slight/minor damage	Probability of moderate damage	Probability of extensive damage	Probability of complete damage

Table 11: Damage Substation Worksheet example

Node	DS_1	DS_2	DS_3	DS_4	DS_5
Substation Node #	Probability of no damage	Probability of slight/minor damage	Probability of moderate damage	Probability of extensive damage	Probability of complete damage

Table 12: Damage Transformers Example Worksheet

Node From	Node To	DS_1	DS_2	DS_3	DS_4	DS_5
Node from #	Node to #	Probability of no damage	Probability of slight/minor damage	Probability of moderate damage	Probability of extensive damage	Probability of complete damage

Table 13: Load Output Example Worksheet

Node	Phase A Real	Phase A Reactive	Phase B Real	Phase B Reactive	Phase C Real	Phase C Reactive
Node #	Phase A real load in W	Phase A reactive load in Var	Phase B real load in W	Phase B reactive load in Var	Phase C real load in W	Phase C reactive load in Var

Table 14: System Data Example Worksheet

Node A	Node B	Length (ft)	Config	Soil	Substation	Voltage	Restore Time
Node from #	Node to #	Length between nodes, in feet	Line configuration, XFM, or Switch	States what type of soil the component is on – 'A', 'B','C','D',' E'	'S' indicates the location of a substation, otherwise, blank	Only filled in for a substation node, 'H','M',' L'	Number of units used to determine the time to restore a given line, based on the length of the line between the nodes

In Table 14, the Restore Time column was created for the optimization model. It was desired to differentiate between the lines on the basis of length, to determine how long it would take to

repair a given line. This number is found by dividing the length in feet given by the user in the initial input file by 50 feet. Distribution poles are typically 40 to 50 feet apart (Crosby, 2011).

3.3. Case study: Testing the algorithm

The algorithm was built in pieces. The original algorithm only used the IEEE 13 node test system, chosen for its smaller size. First, the fragility curves were built, then checked against an example in HAZUS technical user manual. Then, the input data was checked, to ensure it was read in properly. Next, the PGA input was added, and converted to a matrix location. This PGA input was then converted to the PGA as seen by the component based off of the soil composition the component is on. All cases work, if the system is homogeneous with one type of soil, as well as if the system rests on all five types of soils. The user must be aware of where each component is in relation to the others when dictating the parameters for the system. These matrix locations correspond with the appropriate probability of damage done for a given component and a given soil type. Where components were located at with respect to nodes was the next hurdle, and it is accomplished by both user inputs and string comparison. When the algorithm was tested against the larger IEEE test node systems, this part of the algorithm caused the most errors. In order for the algorithm to determine where a transformer is in the system, it looks for the term "XFM-1." When it finds this term, it removes the row containing all of the information and classifies the information as belonging to a transformer. All transformers are assumed to be low voltage transformers and outputs data based upon the substation information. This is an over approximation of the damage state the transformer is likely in, however, there was no available data to build a fragility curve solely for the transformer. This assumption was made knowing transformers are the most susceptible part of a substation and highly influenced the standard mean and deviation values for the substation. The algorithm relies on the input being in the exact format as described in Table 2 and Table 4.

Finding where a substation is located is slightly easier. The 'S' is searched for, and the node number as listed in Column 1 is used to create a new matrix, comprised of solely those nodes which have a substation. The IEEE test node system table are not standard in their nomenclature. The 123 node system in particular does not include all of the nodes in the system. The algorithm user must be aware of these limitations and ensure the desired input is in the required format. Once the components have been sorted, the soil conditions are found. The algorithm correlates the system input data with the corresponding damage probability states. These correlations are output in Table 10 - Table 12. Next, the loads were all multiplied by 1000 because the optimization problem requires the loads to be in base units. The lengths between nodes were divided by 50 in order to determine the time units for restoration. The loads are then output in Table 13, and the restoration time data in Table 14. The last piece of the algorithm to be made was asking the user if all the components were seismically anchored or if they used standard anchors. The difference between what is pulled due to this input is the fragility curve being referenced for damage assessment. Otherwise, the two options are identical.

This algorithm was originally tested on the IEEE 13 node test system. Once it was verified as working as desired, it was then tested on the 34 node, 37 node and 123 node systems. Testing was completed for each smaller system before being performed on a larger system. The largest issue was in standardization of formatting between the different test node system inputs. For a user using this on a non-IEEE system, this will likely be a big issue as well. The inputs must be done as specified in Table *2* and Table 4, otherwise the algorithm will either not work due to errors, or give erroneous results.

3.4. Results: verifying the algorithm

The algorithm was verified by looking at the output data and comparing it with known quantities. The fragility curves were built in both MATLAB and Excel. The MATLAB results were manually cross-references with the Excel quantities. The Excel quantities had been verified against the example found in the HAZUS technical user manual. The component break outs were manually verified with cross-referencing from the algorithm output to the IEEE test node system input. As stated in Section 3.3, various test scenarios were run. The base IEEE system used was the IEEE 13 node test system, with an additional substation added to ensure the substation sort part of the algorithm worked. The initial input for all four test cases to be examined can be seen in Table 15. The only difference between Table 15 and the input the algorithm read in are Columns 5 and 6. For the algorithm read in file, only one of these columns can exist. Otherwise, the algorithm will produce erroneous results. The input PGA for all four cases was 0.5. The multisoil scenario shown in this thesis is not realistic. Most distribution systems have one or two different soil types. An example of this can be found in Seattle. City planners have modified the landscape to such an extent that parts of the city are built on filled earth, resulting in soil conditions much like those found in Mexico City. Other parts of the city are built on undisturbed earth. The filled areas will transmit energy differently than the undisturbed earth. In addition, when designing the multisoil scenario, care was not taken to ensure the soil types matched with the given nodes. The user must ensure the soil conditions and nodes match for their system. The multisoil scenario was chosen to show capability of the algorithm.

Table 15: Test Case input for both single and multisoil conditions

Line Segment Data							
Node A	Node B	Length(ft.)	Config.	Soil-Single	Soil – Multi	Substation	Voltage
632	645	500	603	A	A		
632	633	500	602	A	B		
633	634	0	XFM-1	A	C		
645	646	300	603	A	D		
650	632	2000	601	A	E	S	L
684	652	800	607	A	E		
632	671	2000	601	A	D		
671	684	300	604	A	C		
671	680	1000	601	A	B		
671	692	0	XFM-1	A	A		
684	611	300	605	A	A		
692	675	500	606	A	B		
700	692	500	601	A	C	S	M

There are two differences between this system and the IEEE 13 node test system, Row 13 and the notation XFM-1 in Row 11. In the IEEE 13 node test system, Row 13 does not exist. The only substation is the one at Node 650. The component between Node 671 and 692 is a switch in the IEEE 13 node test system, not a transformer. The results of a test with all components being both seismically anchored and with standard anchors and on the same soil conditions can be seen in Table 16. This table shows the distribution system results. The entire table must be examined as a whole, as opposed to column by column or line by line. The results for each component is the same, which is expected given these components are identical. The seismically anchored components have a greater probability of no to minimal damage whereas the standard components, or unanchored components, have a greater probability of more amounts of damage, and a smaller probability of slight to no damage. For the seismically anchored components, there is an 11.7% probability of being in Damage State 1, or incurring no damage to the system. With the standard components, there is only a 2.1% probability of being in Damage State 1.

There is a greater probability of being in a lower damage state when seismically anchored components are utilized. There is a 38.3% probability of the seismic system being in Damage State 2, or incurring damage to 4% of the distribution circuitry, while there is a 14.8% change of being in this damage state for the standard system. Both systems have the highest probability of being in Damage State 3, or incurring damage to 12% of the distribution system circuitry. The seismic system has a 50% probability, while the standard system has an 82.5% probability of being in this damage state. The seismic system has no probability of being in Damage State 4, while the standard system has a 0.7% probability of incurring damage to 50% of all circuits. Neither system has a probability of being in Damage State 5, with damage to 80% of the distribution system circuitry.

Table 16: Results for both seismic and standard distribution system components with the same soil type

		Seismic Results					Standard Results				
Node from	Node to	ds1	ds2	ds3	ds4	ds5	ds1	ds2	ds3	ds4	ds5
632	645	0.117	0.383	0.500	0.0	0.0	0.021	0.148	0.825	0.007	0.0
632	633	0.117	0.383	0.500	0.0	0.0	0.021	0.148	0.825	0.007	0.0
645	646	0.117	0.383	0.500	0.0	0.0	0.021	0.148	0.825	0.007	0.0
650	632	0.117	0.383	0.500	0.0	0.0	0.021	0.148	0.825	0.007	0.0
684	652	0.117	0.383	0.500	0.0	0.0	0.021	0.148	0.825	0.007	0.0
632	671	0.117	0.383	0.500	0.0	0.0	0.021	0.148	0.825	0.007	0.0
671	684	0.117	0.383	0.500	0.0	0.0	0.021	0.148	0.825	0.007	0.0
671	680	0.117	0.383	0.500	0.0	0.0	0.021	0.148	0.825	0.007	0.0
684	611	0.117	0.383	0.500	0.0	0.0	0.021	0.148	0.825	0.007	0.0
692	675	0.117	0.383	0.500	0.0	0.0	0.021	0.148	0.825	0.007	0.0
700	692	0.117	0.383	0.500	0.0	0.0	0.021	0.148	0.825	0.007	0.0

The results for the multisoil condition are more exciting. These results are shown in Table 17 for the substation nodes to illustrate the system knows to pull out the information for these nodes. In addition, the substations are not the same voltage level. The substation located at Node 650 is a low voltage substation located on Soil Class E, soft clay soil. The substation

located at Node 700 is a medium voltage substation located on Soil Class C, very dense soil and soft rock. Substations, particularly the medium and high voltage substations, tend to incur more damage during an earthquake due to the equipment footprint. The probability of the damage states as shown in Table 17 illustrate this. The substation located at Node 650, a low voltage substation, has lower probabilities of being in higher damage states than the substation located at Node 700, which was modeled as a medium voltage substation. Also, the seismically anchored substations have higher probabilities of being in lower damage states than the unanchored substations.

Table 17: Results for both seismic and standard substation components with different soil types

	Seismic Results					Standard Results				
Node	ds1	ds2	ds3	ds4	ds5	ds1	ds2	ds3	ds4	ds5
650	0.058	0.154	0.288	0.438	0.062	0.028	0.108	0.105	0.651	0.107
700	0.022	0.060	0.103	0.614	0.200	0.004	0.030	0.067	0.399	0.500

Again, the seismic components show a greater probability of lesser amounts of damage being done, no matter the soil conditions or voltage level. As can also be seen from Table 16, the transformers are not mentioned. These results, for the multisoil conditions, are shown in Table 18.

Table 18: Results for both seismic and standard transformer components with different soil types

		Seismic Results					Standard Results				
Node from	Node to	ds1	ds2	ds3	ds4	ds5	ds1	ds2	ds3	ds4	ds5
671	692	0.081	0.199	0.324	0.361	0.036	0.042	0.153	0.148	0.596	0.062
633	634	0.043	0.118	0.246	0.497	0.096	0.019	0.076	0.072	0.669	0.164

The transformers allow for a true comparison of the impact soil conditions may have on the components. The transformer located between Node 671 and Node 692 is on Soil Class A, hard rock, while the transformer located between Node 633 and Node 634 is on Soil Class C, very dense soil and soft rock. Again, it can be seen the seismically anchored components have a

higher probability of being in a lower damage state than the unanchored components. The transformer located on the Soil Class A also has a higher probability of being in the lower damage states than the transformer located on Soil Class C. This is due to the way the seismic energy moves through the earth.

The final abstract for this system, shown for the single soil condition with seismic components, can be seen in Figure 19.

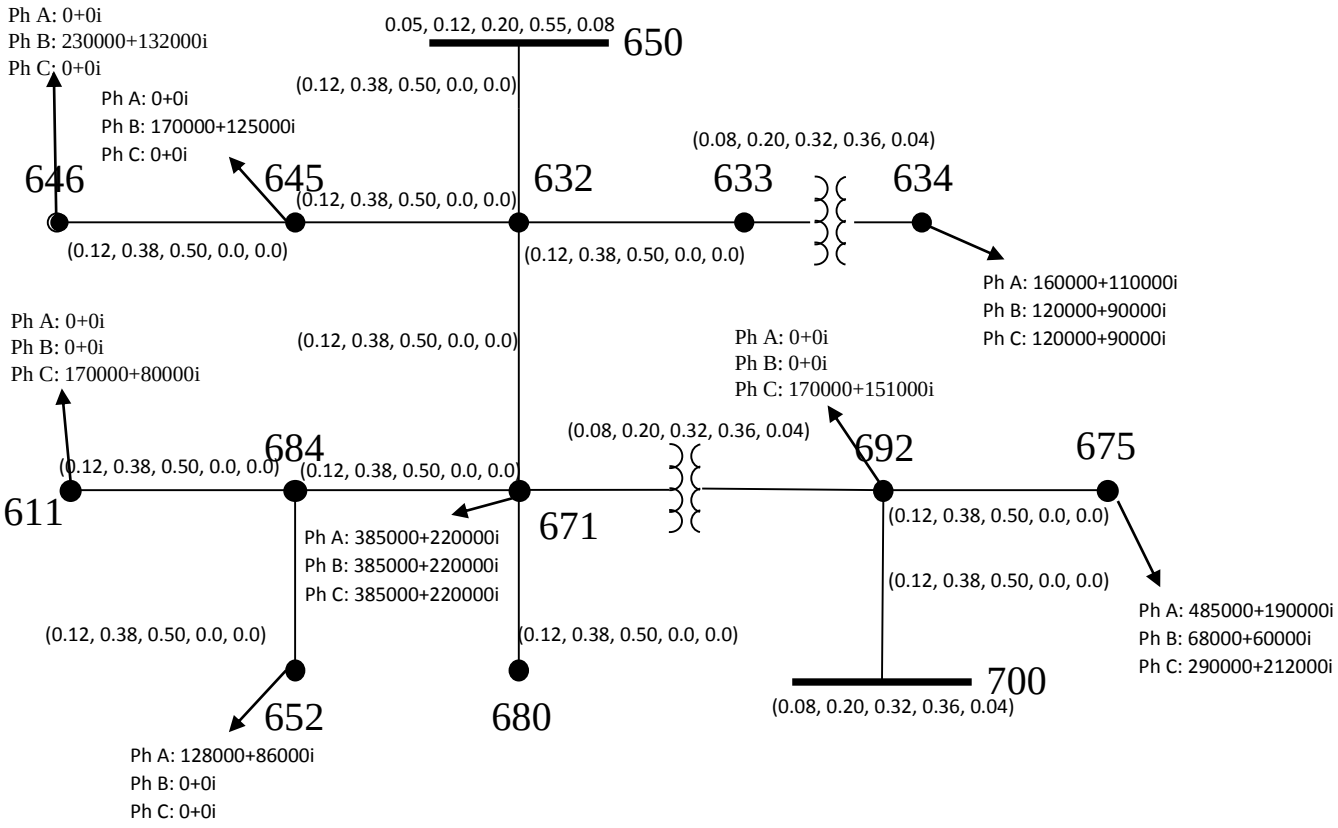

Figure 19: Abstract diagram output of seismically anchored distribution system on single soil type

This system is located on the same soil, Soil Type A. It has a low voltage substation located at Node 650 and a medium voltage substation located at Node 700. The two transformers are modeled as low voltage substations, which is an over approximation, however, no available data

used to determine the fragility curve for the transformer could be found. The lines damage state probabilities are all the same due to the same soil conditions. The nodes which have loads are shown in Figure 19.

4. Conclusions

Natural disasters cause upheaval and destruction by their very nature. The harm caused in their aftermath is unavoidable due to a natural disaster's unpredictable nature. Reducing the harm a populace suffers in the wake of a natural disaster has economic and political repercussions for the affected area. There are steps which can be taken to limit the length of time harm will be suffered by the population affected by a natural disaster – both pre and post natural disaster. Pre-natural disaster steps can include determining where spare parts should be stored, crew training, and what type of component anchorage to use. This research looked into how to determine the probable damage state the components of a distribution system could be in with the earthquake strength as the input. It provides an abstract graph detailing the probability an electrical distribution system component is in a given damage state in the wake of an earthquake. The algorithm created can be used for any distribution system, not just the IEEE test node systems, provided the input format is followed as given in this document.

This abstract graph will then be used to determine the optimal path to restoration. While processing the data, the optimization code determines the probability of damage a given component in the system experiences based off of the probability of the component being in a given damage state as output by this algorithm. An optimization is then performed to minimize the amount of time spent repairing the incurred damage, weighted by load amount and based upon the probability of the amount of damage experienced by the system and the availability of a utility's resources. The results of this optimization can be then used by city planners and officials to help reduce the amount of harm done to their local population, both economically and physically, due to the electrical system being out after an earthquake.

5. Future Work

There is ample opportunity for additional research with this problem. The first is to build a component by component fragility curve for the distribution system consisting of the poles and wires bringing power to businesses and residences. These pieces of the electrical distribution system are considered some of the most reliable and least affected by an earthquake. As such, the fragility parameters utilized in this research are parameters for the entire distribution system as opposed to a line by line or node by node parameter. Understanding how the various parts of the substation react during the natural disaster is also a next area for research. MCEER has begun this avenue, after exhausting ways of making transformers more earthquake resistant. There are countless other pieces and parts found within a substation which are also vulnerable to the earth's movements. In addition, this research could not find fragility information on transformers, only information for the entire substation. The fragility information used to create the distribution circuitry did not include transformers as a potential input. When the results are displayed, the probability amount of damage for a transformer is the same as that for a substation, which is an incorrect assumption. To have fragility data for a transformer would be preferred for an accurate calculation of the probability of damage.

In addition, ground attenuation is not considered in this algorithm. The entire system feels the same amount of seismic energy. For a small system, this is a valid assumption. However, as a system grows larger, this assumption may become invalid based upon where the earthquake's epicenter is located. Load importance factors are not considered either. The desire by officials to get certain areas, such as hospitals, emergency shelters, and control centers, operating smoothly first is not taken into account. Costs are also not included. Future work can

also include determining if it is worth the expense to upgrade the components' anchorage for a system.

With regards to the developed algorithm, it can be expanded to take into account other natural disasters, such as hurricanes, floods, and ice storms. In the course of this research, they were examined with regards to the amount of damage done to a given population, not with specific research towards the amount of damage caused to the electrical system.

References

Abi-Samra, N. & Henry, W., 2011. Actions Before...and After A Flood. *IEEE Power & Energy Magazine*, 2011 February, pp. 52-58.

American Society of Civil Engineers, 2010. *ASCE 7-10: Minimum Design Loads for Buildings and Other Structures*, Reston, VA: American Society of Civil Engineers.

Anon., 2006. *Western Region Geology and Geophysics Science Center.* [Online]
Available at: http://geomaps.wr.usgs.gov/archive/socal/geology/inland_empire/socal_faults.html
[Accessed 13 02 2015].

Anon., 2013. *A Stronger, More Resilient New York: Utilities*, New York City: New York City.

Anon., 2013. *Economic Benefits of Increasing Electric Grid Resilience to Weather Outages*, Washington D.C.: Executive Office of the President.

Anon., n.d. *Kobe Earthquake.* [Online]
Available at: http://www.georesources.co.uk/kobelow.htm
[Accessed 02 December 2014].

Berkeley, A. & Wallace, M., 2010. *A Framework for Establishing Critical Infrastructure Resilience Goals*, s.l.: National Infrastructure Advisory Council.

Berman, J., 2014. *Thomas & Marilyn Nielsen Associate Professor of Structural Engineering and Mechanics, University of Washington* [Interview] (August - November 2014).

Bustos, A., 2014. *Lineman Supervisor, Department of Public Utilities, Los Alamos County* [Interview] (February 2014).

ConEdison, 2013. *Fortifying the Future & Summer Preparedness.* New York City: conEdison.

Crosby, A., 2011. *Special Research Topic Report on Current Practice in Utility Distribution Poles and Light Poles*, s.l.: s.n.

Department of Homeland Security and Federal Emergency Management Agency, n.d. *Earthquake Model: Hazus-MH 2.1 Technical Manual.* Washington, D.C.: Department of Homeland Security and Federal Emergency Management Agency Mitigation Division.

Distribution System Analysis Subcomittee, n.d. *IEEE 13 Node Test Feeder.* New York: IEEE Power Engineering Society.

Distribution System Analysis Subcommittee, n.d. *IEEE 123 Node Test Feeder.* New York: IEEE Power Engineering Society.

Distribution System Analysis Subcommittee, n.d. *IEEE 34 Node Test Feeder.* New York: IEEE Power Engineering Society.

Distribution System Analysis Subcommittee, n.d. *IEEE 37 Node Test Feeder.* New York: IEEE Power Engineering Society.

Eidinger, J. & Tang, A. K., 2012. *Christchurch, New Zealand Earthquake Sequence of Mw 7.1 September 04, 2010; Mw 6.3 February 22, 2011; Mw 6.0 June 13, 2011: Lifeline Performance,* s.l.: American Society of Civil Engineers.

Ersoy, S., Feizi, B., Ashrafi, A. & Saadeghvaziri, M. A., 2008. *Seismic Evaluation and Rehabilitation of Critical Components of Electrical Power Systems,* Buffalo: Multidisciplinary Center for Earthquake Engineering Research.

Ersoy, S., Feizi, B., Ashrafi, A. & Saadeghvaziri, M. A., 2008. *Seismic Evaluation and Rehabilitation of Critical Components of Electrical Power Systems,* Buffalo: MCEER.

Fichter, L. S. & Baedke, S. J., 2000. *Plate Tectonic Theory: Plate Boundaries and Interplate Relationships.* [Online]
Available at: http://csmres.jmu.edu/geollab/vageol/vahist/plates.html
[Accessed 2015 January 9].

Flynn, S. E. & Burke, S. P., 2012. *Powering America's Energy Resilience,* s.l.: The Center for National Policy.

Heimgartner, C., 2014. *Snohomish PUD Assistant General Manager* [Interview] (November 2014).

IEEE Power Engineering Society, 2005. *IEEE 693: IEEE Recommended Practice for Seismic Design of Substations ,* New York: IEEE.

Kempner, L., 2007. *Substation Structure Design Guide.* s.l.:American Society of Civil Engineers.

Kempner, L., 2013. *BPA structural engineer and seismic mitigation program manager* [Interview] (November 2013).

Knight, B. T. & Kempner, L., 2004. *A Utility's Approach to Seismically Hardening Existing High-Voltage Electrical Transmission Substation Equipment.* Vancouver, B.C., Canada, World Conference on Earthquake Engineering.

Lamonica, M., 2012. *OnEarth Blog.* [Online]
Available at: http://archive.onearth.org/blog/to-make-the-grid-more-resilient-break-it-into-islands
[Accessed September 2013].

Lavergne, M., 1989. *Seismic Methods.* 1 ed. Paris: Editions Technip.

Lowry, H., 2014. *myfoxla.com.* [Online]
Available at: http://www.myfoxla.com/story/24448460/a-look-back-at-the-northridge-quake-facts-figures
[Accessed 02 December 2014].

Maliszewski, P. & Perrings, C., 2012. Factors in the resilience of electrical power distribution infrastructures. *Applied Geography,* 32(2), pp. 668-679.

Mili, L., 2011. *Taxonomy of the Characteristics of Power System Operating States,* Falls Church, VA: National Science Foundation.

Murota, N., Feng, M. Q. & Liu, G.-Y., 2005. *Experimental and Analystical Studies on Base Isolation Systems for Seismic Protection of Power Transformers,* Buffalo: MCEER.

Ouyang, M., 2014. Review on Modeling and Simulation of Interdependent Critical Infrastructure Systems. *Reliability Engineering and System Safety,* Volume 121, pp. 43-60.

Ouyang, M. & Duenas-Osorio, L., 2014. Multi-dimensional Hurricane Resilience Assessment of Electric Power Systems. *Structural Safety,* Issue 48, pp. 15-24.

Ouyang, M., Duenas-Osorio, L. & Min, X., 2012. A Three-Stage Resilience Analysis Framework for Urban Infrastructure Systems. *Structural Safety,* Volume 36-37, pp. 23-31.

Pacific Northwest Seismic Network, n.d. *Plate Tectonics.* [Online]
Available at: http://pnsn.org/outreach/about-earthquakes/plate-tectonics
[Accessed 8 January 2015].

Porter, K., Kennedy, R. & Bachman, R., 2007. Creating Fragility Functions for Performance-Based Earthquake Engineering. *Earthquake Spectra,* 23(2), pp. 471-489.

Rathje, E. M., 2010. *Soil Amplification and Topographic Effects.* Austin, TX: University of Texas at Austin.

Rudnick, H. et al., 2011. Disaster Management. *IEEE Power & Energy Magazine,* 23 February, pp. 37-45.

Schneider, K., 2014. *Affiliate Assistant Professor, University of Washington* [Interview] (January 2014).

Shinozuka, M., Cheng, T.-C., Feng, M. Q. & Mau, S.-T., 1999. *Seismic Performance Analysis of Electric Power Systems,* Buffalo: Multidisciplinary Center for Earthquake Engineering Research.

Southern California Earthquake Data Center, n.d. *The Distribution of Earthquakes.* [Online]
Available at: http://scedc.caltech.edu/Module/s2act08.html
[Accessed 21 January 2015].

Tan, Y., 2014. *PhD Candidate, University of Washington* [Interview] (24 December 2014).

U. S. Department of the Interior, 2014. *Earthquake Facts & Earthquake Fantasy.* [Online]
Available at: http://earthquake.usgs.gov/learn/topics/megaqk_facts_fantasy.php
[Accessed 23 January 2015].

U.S. Department of the Interior, 2012. *Pacific Northwest Geologic Mapping and Urban Hazards.* [Online]
Available at: http://geomaps.wr.usgs.gov/pacnw/resfzno.html
[Accessed 9 January 2015].

Wikipedia, n.d. *Juan de Fuca Plate.* [Online]
Available at: http://en.wikipedia.org/wiki/Juan_de_Fuca_Plate
[Accessed 9 January 2015].

Wong, C. J. & Miller, M. D., 2010. *Guidelines for Electrical Transmission Line Structural Loading.* 3rd ed. s.l.:American Society of Civil Engineers.